Classification and Segmentation of COVID-19 from CT and X-ray Images using Deep Architectures

Author

Hafiz Muhammad Sarmad Khan

NUST CEME 00000274869

Supervisor

Dr. Arslan Shaukat

Department of Computer and Software Engineering

College of Electrical and Mechanical Engineering

National University of Sciences and Technology (NUST)

Islamabad, Pakistan

Classification and Segmentation of COVID-19 from CT and X-ray Images using Deep Learning Architectures

Author

Hafiz Muhammad Sarmad Khan

NUST CEME 00000274869

A thesis submitted in partial fulfillment of the requirements for the degree of

MS Computer Engineering

Supervisor

Dr. Arslan Shaukat

Thesis Supervisor's Signature: _____

Department of Computer and Software Engineering

College of Electrical and Mechanical Engineering

National University of Sciences and Technology (NUST)

Islamabad, Pakistan

Declaration

I certify that the research titled *"Classification and Segmentation of COVID-19 from CT and X-ray Images Using Deep Learning Architectures"* is my own work. The work was not submitted for assessment elsewhere. The material utilized from external sources has been acknowledged / referred correctly.

Hafiz Muhammad Sarmad Khan

NUST CEME 00000274869

Language Correctness Certificate

This thesis has been proofread by an English expert and is error-free in terms of typing, syntax, semantics, grammatical structure and spelling. The format of the thesis is also prescribed by the university.

Hafiz Muhammad Sarmad Khan

NUST CEME 00000274869

Copyright Statement

Acknowledgment

I am immensely grateful to Allah Almighty for providing me with the patience, direction, and capacity to complete this work. Without HIS blessings I could not have completed my thesis. Indeed Allah is the most merciful and worthy of praise.

I would like to express my gratitude to my supervisor Dr.Arslan Shaukat for their guidance, valuable suggestions and moral support in the entire duration. It's a blessing to have such great people as mentor for research

I am also thankful to the entire thesis committee: Dr. Muhammad Usman Akram and Dr. Sajid Gul Khawaja for their tremendous support and cooperation

My acknowledgment would be incomplete without mentioning my beloved parents without whom I am nothing and who have supported me in every second of my life. I would also like to thank my friends who have always supported me and especially during the research work

Finally, I'd want to convey my thanks to each and every one of my friends and all the individuals who have encouraged and supported me throughout the entire duration.

This thesis is dedicated to my wonderful parents and cherished friends, whose unwavering support and collaboration helped me achieve this magnificent goal.

Abstract

COVID-19 has become a significant challenge, with numerous human beings losing their lives every day. Not only a certain country is involved with this outbreak, but even the world has suffered because of the corona virus. Computed Tomography (CT) and X-ray images of lungs are the best resources for COVID-19 screening. It is essential to quickly and accurately identify and segment COVID-19 from CT and X-rays to aid in diagnostic and patient monitoring. Technology today has revolutionized the world by using artificial intelligence to replace manual process with automated machines, which enable the system to imitate the human brain by making wise decisions based on experience. Motivated by this, our work proposes to use convolutional neural networks (CNN) based models for designing computer aided diagnosis (CAD) system which differentiates between COVID-19 and normal healthy lungs from both CT and X-ray images. An automated system has also been proposed which segments the COVID-19 disease form the radiological images of lungs using deep learning networks. For classification, two datasets of lungs X-ray and two of CT images have been utilized. Similarly, two CT lungs image datasets are used for segmentation. Various pre-trained networks are employed for classification such as VGG (16, 19), Densenet (121), Resnet (50, 50 V2, 101 V2), Mobile net (V2), Xception Inception (V3, Resnet V2), Efficient net (B0) and Nasnet (Large). For segmentation, main architectures used are: Unet, Link Net, Pyramid Scene Parsing Network (PSP Net), and Feature Pyramid Network (FPN). The pre-trained feature extraction networks used as encoders with these segmentation architectures are: Efficient Net, MobileNet V2, Seresnet 101, Densenet 121, VGG-19, and Inception Resnet V2. A thorough testing of all well-known deep architectures has been done and a comparative analysis of these architectures has also been performed. Resnet V2 and VGG-16 has proven to be effective in accurately classifying the COVID-19 from healthy images giving an average accuracy in the range of 95% to 98% on the four X-ray

and CT image datasets. In segmentation, Unet, FPN and Link Net with backbones of MobileNet V2, Densenet 121 and Inception Resnet V2 have reported highest F1-Scores of 77% to 98.6% on the two CT image datasets. Our achieved results are competitive and higher as compared to previous reported results in literature on the four datasets of classification and two datasets of segmentation.

Keywords: *COVID-19, Deep learning, Image Classification, Image Segmentation, CT, X-rays.*

Contents

List of Figures

List of Tables

Chapter 1

Introduction

Many formerly human-dependent processes have been automated by technology, which has revolutionized the environment. Equipment's & technology is present in all spheres of life, from the simplest gadget such as a calculator to massive factory machines. Machines are programmed to execute a series of instructions/commands in order to complete tasks without the need for human intervention. Artificial Intelligence (AI) has revolutionized the world beyond our imagination as technology advances. Machines are trained to imitate the human brain by learning from experience utilizing AI. Usefulness of AI in the area of medicine has piqued interest, & the first attempt to create a Computer Aided Design (CAD) was made in the 1960s. Artificial intelligence (AI) methods have been utilized in medicine to automate the diagnosis of a variety of diseases. Automatic disease identification has been a hot subject, with many experts contributing to the field by proposing a variety of CAD systems. Such systems assist radiologists in detecting diseases in less time and often serve as a second opinion for radiologists in making the best pathology decisions. However, in order for such systems to make unsupervised decisions, transfer learning is required, which necessitates a vast amount of data, and most medical image datasets have been found to be imbalanced. As a consequence, this research suggests a systematic comparison of deep learning models for CAD systems that employ image classification to distinguish between COVID-19 and normal healthy human lungs in CT scans and x-ray images as well as image segmentation to estimate COVID-19's location in CT images.

1.1 Motivation:

Ever since the emergence of coronavirus, a lot of individuals & human beings have died from the COVID-19 breakout. Although as most of the victims and mortalities were reported in China, the World Health Organization on 30 January 2020 proclaimed this outbreak as a Public Health Emergency of International Concern and a pandemic on 11 March 2020 [1]. It's cure & medication can take a couple of months due to its clinical experimentation & trials on human being of various age group before acceptance and the treatment may further be postponed due to the virus's potential genetic mutations [2]. New born babies, children, and elderly patients are affecting by SARS-CoV-2. To save more lives, an early diagnosis of any kind of disease, whether contagious and non-contagious is extremely a supreme task. An early screening and fast diagnosing procedure can avoid the spread of epidemic diseases, speed up the related diagnosis and cost-efficient. However, in order for such systems to make unsupervised decisions, transfer learning is required, which necessitates a vast amount of data, and as this disease is relatively new to the world, there most medical image datasets have been found to be imbalanced. As a result, this research suggests systematized comparison of deep learning models for CAD systems that use image classification to make a distinction between COVID-19 infected individuals and healthy people in CT and x-ray images, as well as image segmentation to determine the position of coronavirus in CT images.

1.2 Problem Statement:

Early diagnosis of any disease, contagious or anti, is vital for effective care and the saving of more lives. An early screening and fast diagnosing process will help prevent the spread of pandemic diseases while also reducing expenses and speeding up the diagnosis process. Many CAD schemes have been suggested for other diseases to date. Since COVID-19 is a novel disorder, the hardest challenge for the researchers is the data availability. Furthermore, the majority of the coronavirus CT and X-ray datasets are inconsistent and unbalanced. As a consequence, the objective of this dissertation is applying various DL strategies in order to develop an effective diagnostic method. Not only the deep learning algorithm will speed up the identification process, but it will also relieve the pressure on doctors and health-care systems.

1.3 Aims and Objectives:

The primary aims of the research being carried out are as follows:

- Inspect and equate previous studies on the automated diagnosis of novel coronavirus (COVID-19) and the detection.
- Gathering datasets for COVID-19.
- Proposing a classification framework for differentiating images of normal and COVID-19 X-rays and CT scans.
- Proposing a segmentation architecture for identifying the region of interest on COVID-19 CT scans.

1.4 Structure of Thesis:

The study carried out introduces the problem, outlines the research conducted, and briefs about the experiments conducted. An overview of the structural organization is given as:

- **Chapter 2** is a study of previous literature on COVID-19 identification by researchers and the lungs which are an essential organs for respiration are briefly described in **Chapter 3** along with their anatomy. COVID-19 and its early prevention are also explored in depth.
- **Chapter 4** will cover in-depth awareness of deep learning and its architectures.
- **Chapter 5** summarizes the suggested architecture and datasets that were utilized. COVID-19 classification in CT scans and X-rays and COVID-19 segmentation in CT scans are the two key modules.
- Datasets and performance metrics that were utilized to evaluate the proposed architecture are outlined in **Chapter 6**. Many of the conclusions, as well as the table of results and figures are discussed elaborately.
- This study is wrapped up in **Chapter 7**, which also outlines the thesis's potential / future goals.

Chapter 2

Novel Coronavirus (COVID-19)

The five vital organs of the human body are the heart, central nervous system, liver, kidney, and lungs. The respiratory system relies on the transfer of Carbon dioxide And oxygen between body and environment. This chapter will cover lung anatomy and imaging methods, as well as a brief presentation to the Novel Coronavirus (COVID-19).

2.1 The Role and Anatomy of Breathtaking Lungs

The lungs are the centre of the respiratory (breathing) process. Every cell in the body necessitates the presence of oxygen in order to survive. As a result, the body must eliminate CO2. This gas is a byproduct of the normal operations of cells. The lungs are built to exchange these gases whenever users take a breath in or out. Let us take a closer look at this complex system[3].

2.1.1 Lungs Anatomy:

This pinkish, spongy organ in the chest usually consists of two upside-down cones. The right lung is divided into three lobes and to make room for the heart, the left lung has just two lobes.

The lungs originate at the bottom of the trachea (windpipe). The trachea is a tube via which oxygen enter and leave the lungs. Each lung is bonded to the trachea called bronchus. In the chest, the tracheal and bronchial passageways form an upside-down "Y". The bronchial tree is named for its "Y".

Bronchial are broken down into narrower bronchi & bronchioles, which are also smaller tubes. These minuscule tubes shoot out into every area of the lungs. They're so little that some are the thickness of a feather. Nearly 30K bronchioles are found in each lung.

The alveoli are a cluster of small air sacs at the end of each bronchiole channel. They resemble like little balloons. There are approximately 600 million alveoli in the lungs. They have a surprising amount of surface space, similar to atennis court, because of the minuscule bubble forms. This signifies that there is enough space for essential oxygen to penetrate the body.

2.1.2 The Respiratory System:

The lungs are vital to the respiratory system. Upper and lower respiratory passageways make up this system.

The upper respiratory consists of the following organs:

- The human mouth and nose
- Pharynx
- The Nasal Chamber
- Larynx

The lower respiratory tract is comprised of the following elements:

- Lungs
- Bronchi and Bronchioles
- Trachea
- Alveoli

When people breathe, different sections of the respiratory system assist the lungs in expanding and contracting. The ribs that surround the lungs, as well as the dome-shaped diaphragm muscle behind them, are included.

2.1.3 Structure of Lungs:

2.1.4 The pathway of breath:

Air reaches the mouth and nose when people respire and travel the pictorial representation can be observed in figure 2.1 [4], while the process is as follows:

- Down the neck and into the trachea.

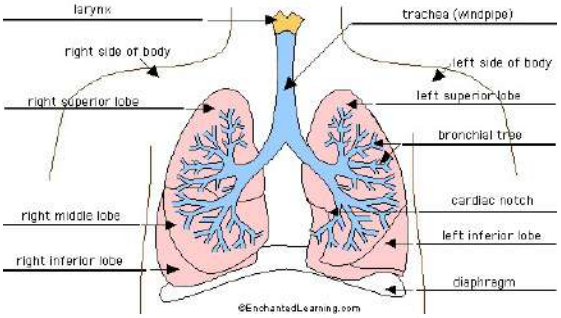

Figure 2.1: Structure of lungs

- The lungs' right and left major bronchi.
- Then it goes into the tiny bronchial airways.
- Into the even smaller bronchi tubes.
- Finally, Into the alveoli.

2.1.5 How lungs can stay healthy:

And as human being exhale air, the alveoli remain partially inflated like a balloon. Surfactant is a fluid produced by the lungs to keep them open. Surfactant also includes fatty proteins that aid in the proper functioning of the lungs.

The lungs disinfect themselves.

Mucus are produced to capture germs and particles. Cilia, thin hairs that cover the airways, and sweep away the mucus. This mucus is normally swallowed without your knowledge. The lungs can produce too much mucus if someone have a respiratory illness.

Macrophages, which are immune cells, are also found in the alveoli. Until germs and irritants will create an infection in your lungs, these cells "kill" them.

2.1.6 Lungs disorder and illness:

A respiratory ailment might be acute or persistent (long term). Certain forms can cause or be an indication of lung illness. Common lung illnesses include the following:

- Asthma
- Bronchitis
- Pneumonia
- Tuberculosis (TB)

2.1.7 Causes of lung disorders and illnesses:

Breathing difficulties may be caused by respiratory or lung conditions. In most countries, they are a frequent cause for doctor visits. A human being can get respiratory illness due to:

- Bacteria
- Virus
- Mold
- Polluted air
- Chemicals
- Stagnant indoor air
- Tobacco, cigarettes
- Allergies like pollen, dust, food

2.1.8 Symptoms to see a doctor:

The American Lung Association refers the following early symptoms of lung infection: "chronic cough, breathing difficulty, chest pain, Sputum in lungs, bloody coughing"

2.1.9 Lungs function test:

If a person suffers from a respiratory illness, they may need scans to determine how well their lungs are doing. They will also aid in the diagnosis of chronic lung disease. For those with chronic illnesses like asthma, some of these tests are normal. The following are some of the most popular lung functioning examinations:

- Arterial blood-gas analysis
- Blood test
- Chest x-ray
- Exhaled nitric oxide test
- Lung diffusion test
- Mucus sample

2.1.10 Lungs treatment:

Some treatments for respiratory issues include:

- Antibiotics
- Anti-viral medication
- Anti-fungal medication
- Heart burn drugs
- Synthetic surfactant drugs
- Immune system medication

2.1.11 Tips for Maintaining Lung Health:

Although the human body has a mechanism in place to keep the lungs safe, there are a few things people can do on a daily basis to either reduce the chance of lung cancer or alleviate symptoms:

- Don't smoke
- Don't chew tobacco
- Acquire a flu and pneumonia vaccination
- Regular aerobic exercises.
- Wash your hands several times a day with soap and water, and so forth.

2.2 Medical Imaging

Medical imaging is defined as the use of imaging tools and methodologies to generate visuals of the human body that may be used to help in patients undergoing treatment. It may also be used to track any chronic illnesses and aid in treatment planning. There are numerous sorts of medical imaging modalities, each one employs a unique technology to generate scans for the reasons indicated below:

2.2.1 CT Scanners:

Using x-rays and computers, computerised tomography often known as a CT scan, may provide a comprehensive image of the interior of the body. This differs from x-rays in that it produces a cross-sectional image of body, similar to that produced by magnetic resonance imaging (MRI), which increases its effectiveness in evaluating soft tissue that an x-ray may miss. They are also capable of projecting skeletons, vital organs, and blood vessels, among other things. The head, neck, back, belly, and sinuses are other routinely examined upper body areas.

2.2.2 MRI Scanners:

MRI scan is a precise cross-sectional representation of a human body's region. It's comparable to a CT, but the image resolution is higher, allowing users to discern tissue differences. The applications are comparable to that of a CT scanner: diagnosis, additional information for treatment planning and continuing therapy monitoring.

2.2.3 Ultrasound:

Ultrasound is a technique which involves strong frequency waves to detect what's happening inside a human organ. It's also referred as a sonogram. Real-time images of newborn children can be generated via ultrasounds.

2.2.4 X-ray:

The use of X-rays to image the inside of the body is a standard practice. It employs x-ray photons from the electromagnetic spectrum. They are used to generate images of limbs to see whether there is any breaking, plus dentists and orthodontists use them to assess teeth. X-rays can also be used to diagnose bone malignancy. It can also be used to diagnose broken bones and choose the best treatment plan.

X-rays are favored by physicians due to their lower expense and lower radiation exposure as compared to CT scans.

The figure 2.2 depicts the various Medical Imaging procedures for lung and thoracic cavity visualization.

2.3 Novel Coronavirus (COVID-19)

Coronaviruses are viruses that cause lung disease. Corona are the spikes on the viral surfaces that form the crowns. SARS, MERS, and the common cold are all caused by coronavirus infections. [5]. SARS-CoV-2 was identified as a novel coronavirus type by the WHO in January 2020. COVID-19 was identified in Wuhan, China, in December 2019 and has since spread globally [6].

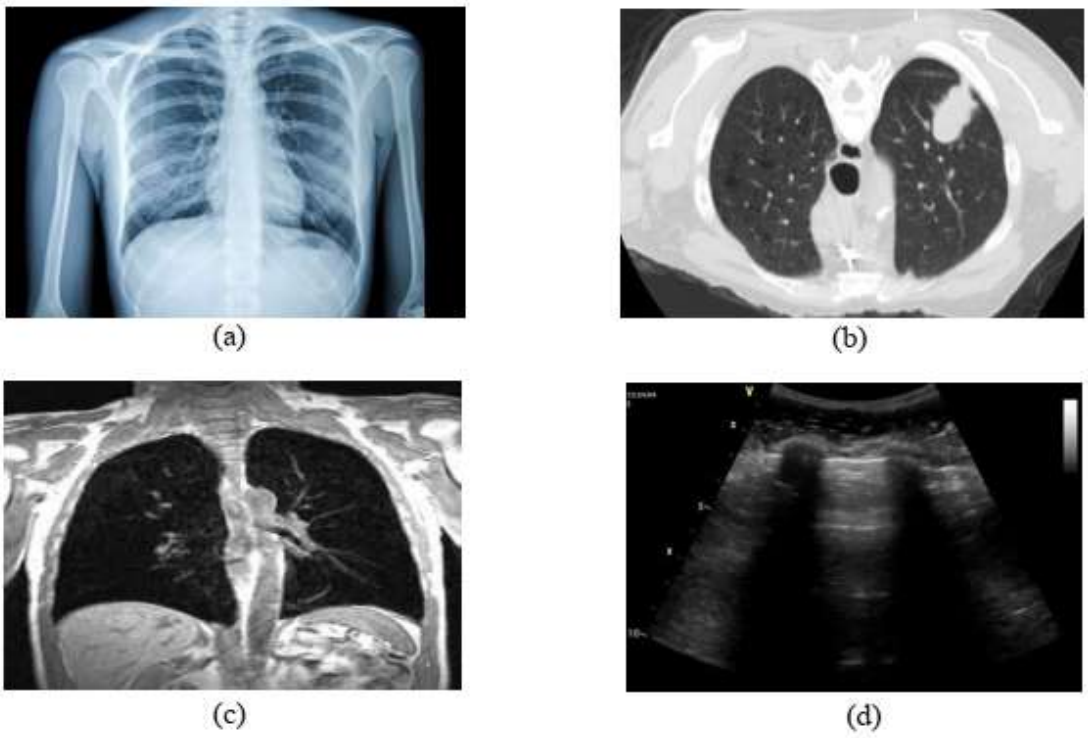

Figure 2.2: Different medical imaging for lung visualization (a) X-ray (b) CT Scan (c) MRI (d) Ultrasound

2.3.1 Causes of COVID-19:

According to the scientists, it's unknown what triggered it. Coronaviruses occur in a range of shapes and sizes. They may be found in a wide range of species notably bats, camels, cats, and cattle.

2.3.2 Risk factor:

COVID-19 will infect anybody, though the majority of infections are minor. The risk of serious illness increases as a person gets older. If someone have the following medical issues like "kidney disease, weak immune system, Sickle cell disease, diabetes, Artery disease", they might be more susceptible to severe illness.

The following conditions may result in severe COVID-19 illness: "asthma, high blood pressure, weak immune system, liver disease, Dementia, damaged lung tissues, Thalassemia" etc.

Any COVID-19-infected children and teenagers develop an inflammatory disorder known as multisystem inflammatory syndrome in infants, according to physicians. Doctors

believe it has everything to do with the infection. It has signs that are related to toxic shock and Kawasaki disease, which induces inflammation in the blood vessels of children.

2.3.3 COVID-19 Early signs:

The following are the primary symptoms:

- Sickness
- Coughing
- Breathing difficulty
- Trouble breathing
- Body aches
- Headache
- Sore throat
- Nausea
- Diarrhea

2.3.4 COVID-19 Diagnosis:

If a person believes they have been infected and are experiencing symptoms like these, they should contact their doctor or the local health department.

- A fever of 100 degrees Fahrenheit or higher
- Coughing
- Difficulty in breathing

Testing services have become more widely accessible in most nations. Some need an appointment, whilst others are easily walk-in.

A swab test is the most commonly used technique. It examines the upper respiratory tract for signs of infection. The person performing the procedure inserts a swab into the nose to collect a sample. The obtained sample is typically sent to a lab to be examined for viral content, though certain locations may offer accelerated testing with results in less than 15 min.

2.3.5 Visual identification of COVID-19 in medical imaging:

Medical imaging has been used to diagnose, monitor, and aid in the care of multiple health problems for over a century including cancer, infectious diseases, heart disease, and neurological disorders. Although there are a variety of imaging procedures available,

chest X-rays, chest computed tomography (CT), and lung ultrasound are the three most often used approaches for examining COVID-19 patients.

These three methods are complementary and provide choices for determining how COVID-19 impacts various organs at various times. Since respiratory symptoms have been found to be among the first signs of COVID-19, they are used on the lung and chest region. Figure 2.3 [7] represents the visual identification of COVID-19 in X-ray, CT and Ultrasound images.

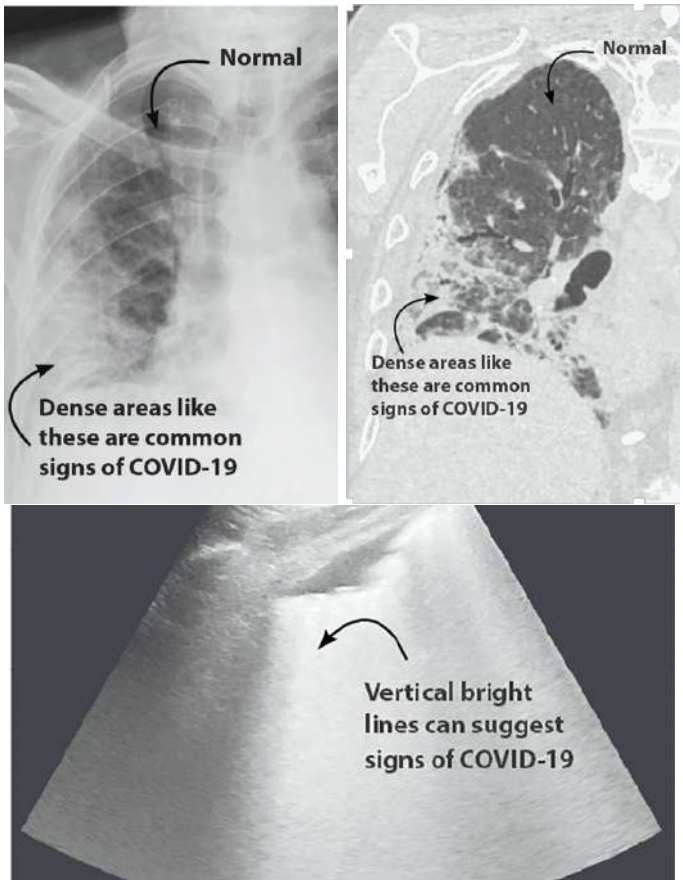

Figure 2.3: Visual identifications for COVID-19 in medical imaging (a) X-ray (b) CT (c) Ultrasound

2.3.6 Prevention:

WHO advises the following strategies to avoid COVID-19 spread:

- Hands should be washed frequently. Use soap and water or an alcohol-based hand rub.
- Maintain a safe distance from somebody who is sneezing or coughing..

- Wear a mask when physical separation is not feasible.
- Keep your hands away from your eyes, nose, and mouth.
- If you are feeling ill, stay at home.

2.3.7 Treatment:

The World Health Organization (WHO) and doctors recommend multiple treatment options for COVID-19 mentioned below:

1. **Self care:**
    - Contact your healthcare provider or the COVID-19 hot line to find out where and when to get a test.
    - If the testing ain't accessible, avoid interactions with individuals and remain at home for 14 days.
    - While you are quarantined, do not attend to work, school, or crowded areas.
    - Maintain a 1-metre distance from others, including family members.
    - Even if you require medical assistance, wear a medical mask to safeguard others.
    - Maintain enough ventilation in the room.
    - Maintain a positive mindset by remaining in touch with friends and family by phone or internet and exercising at home.
2. **Medical Assistance:**

    Scientists all across the globe are working on developing COVID-19 treatments.
    - Individuals who are chronically unwell and at risk of complications illness, appropriate preventative therapy necessitates the use of oxygen, as well as more specialised respiratory aid, such as ventilation.
    - Dexamethasone may help individuals with severe and life-threatening ailments spend less time on a ventilator and live much longer life.

2.3.8 When to consult a doctor:

Keep indoors and watch for signs for the next 14 days if a person find that they have been exposed to somebody who has positive tests for the virus or has been infected with it, according to UCI Health infectious disease experts. If a person develops the distinctive signs of COVID-19, such as fever, shortness of breath, or a new cough, they should contact their doctor. The doctor will decide if they need to see a doctor, be checked, go to a hospital center right away, or take care of themselves at home.

2.4 Summary:

It can be concluded that Covid-19 has evolved into a huge issue, with many people dying every day. This outbreak has affected not just a single country, but also the whole planet. Several viruses, including SARS, MERS, the flu, and many others, have received vaccines in the last decade, although they have only been used for a few days or months. Vaccines are accessible since many scientists work with viruses of this type, and only a handful have been identified. Many additional forecasts, such as plasma therapy, chest and X-ray imaging, have come into play in the meanwhile. Every day, Covid-19 steals the lives of individuals, and the disease's diagnosis is prohibitively expensive in the context of a country, state, and patients.

Chapter 3

Literature Review

Worldwide, more than 100 million instances of coronavirus disease 2019 (COVID-19) (formerly known as the 2019 novel coronavirus) have been confirmed since December 2019 in Wuhan, China (SARS-CoV-2). As a consequence, several people died. However, considering the fact that the vast majority of COVID-19 incidence and fatalities occurred in China, the WHO has designated this a global emergency. Also, hospitalized patients and health workers are at risk for nosocomial infection, as are asymptomatic carriers [8, 9].

Due to the COVID-19, a huge epidemic has now occurred globally, affecting the lives of many people globally. According to the worldmeter.com, the outbreak had infected over million of individuals, resulting in over numerous deaths.

Early diagnosis of any illness, contagious or non-infectious, is vital for effective care and the saving of more lives. A rapid diagnosis and screening procedure can assist to prevent the spread of pandemic illnesses such as SARS-CoV-2 while also saving money and speeding up the diagnosis and treatment. As computer technology advances, a computer aided device (CAD) can assist in diagnosis of illness from chest X-rays and CT scans, as well as provide the radiologist with a second opinion about their diagnosis.

The goal of this literature review is to provide a comprehensive understanding of the uses of machine learning and deep learning in tackling the issues posed by COVID-19. As a result, this literature review will cover some of the concepts and approaches that AI have addressed so far. Classification and segmentation are the techniques and approaches used, and they have been validated on publicly accessible datasets.

3.1 Deep learning classification research on COVID-19

To construct a medical image classification model, features are extracted from the dataset and a classifier is trained on those features to distinguish between normal and abnormal instances, much like any other classification issue. COVID-19 grouping has been the subject of many studies. The following is a summary of the published work in this area.

The article [10] reports *Tuan D. Pham's* research using 16 pre-trained COVID-19 Convolutional Neural Networks based on a massive public database of CT scans from COVID-19 and non-COVID-19 patients. The database comprises 349 COVID-19-positive CT pictures from 216 patients, as well as 397 non-COVID-19 positive CT scans. These CT scans are from COVID19 studies on medRxiv, bioRxiv, and other journals. The dataset was split into two parts, training and testing. The findings revealed a 93% using data augmentation and a 96% accuracy without data augmentation.

Covid versus No-Findings: *T.Ozturk, M.Talo* et al [11] provided a framework for binary and multi-class classification. Their work used the Dark Net model as a classifier for a "you only look once (YOLO)" real-time item identification system. COVID-19 was found using X-ray pictures from two different sources. Their model correctly classified binary classes 98.8% and multi-class instances 87.0%.

COVID-19 infection detection using Deep Convolutional Neural Networks (CoroNet) was proposed by *Asif Iqbal Khan* et al [12]. An Xception architecture was used to build the recommended model, that was pre-trained on the Imagenet database and then trained end-to-end on COVID-19 and other lung pneumonia X-ray images. CoroNet was trained and evaluated on the provided dataset, with an overall accuracy of 89.6% for 4-class cases (COVID vs Pneumonia bacterial vs pneumonia viral vs normal). The proposed model achieved 95% classification accuracy in 3-class classification (COVID, Pneumonia, Normal) and 98% in binary classification (COVID vs normal).

Tanvir Mahmud introduced CovXNet [13], a deep convolutional neural network-based architecture that effectively extracts varied properties from chest X-rays. The proposed method was five-fold cross-validated. CovXNet detects COVID-19 and other pneumonia using chest X-rays. Effective element - wise convolution was used instead of conventional convolution. Extensive testing on two datasets achieves 97.4% accuracy for binary class

and 90.2% accuracy in multi class classification.

In [14], *Alejandro R. Martinez* presented Multi-Source Transfer Learning (MSTL) as an extension to classical Transfer Learning for the classification of COVID-19 using four pre-trained models from Tensorflow's Kera's API: ResNet50V2, ResNet101V2, DenseNet121, and DenseNet122. The models outperformed baseline ImageNet fine-tuned models thanks to their multi-source fine-tuning strategy. Moreover, he also suggested an unsupervised label creation method for their Deep Residual Networks, which improves their efficiency. The model was able to reach a 89% accuracy rate.

COVID-19 classification in CT images using DL-based approaches was suggested by *Hammam Alshazly* et al [15]. These tests were performed on the two datasets with the most Ct scan images accessible to date, "SARS COV 2 and COVID-19 CT". To achieve the best results, they tested numerous designs and created custom inputs for each network. Their models had average accuracy of 98% and 92%, respectively.

In [16], *Bin Liu* et al devised a lesion-attention deep neural network that extracts two types of valuable information for the annotations from the textual radiological report that arrives with each CT image: One is an indication of whether a COVID-19 case is positive or negative, and the other is a description of five lesions on CT scans that are compatible with positive instances.According to the experimental results, the area under the curve, sensitivity, specificity, and accuracy for COVID-19 diagnosis were 94.0 percent, 88.8 percent, 87.9 percent, and 88.6 percent, respectively.

To annotate each CT image, *Bin Liu* et al developed a lesion-attention deep neural network that retrieves two forms of useful information: They describe five lesions on CT scans that are consistent with positive COVID-19 cases. The experimental findings showed that COVID-19 diagnosis had a 94% AUC, 88% sensitivity, 87% specificity, and 88% accuracy [16].

In [17], *D. M. H. Nguyen* et al suggested a novel strategy for improving COVID-19 diagnosis by making use of deep learning-based systems. Unlike previous research, they were motivated by radiologists' decisions while evaluating COVID-19 patients and as a result, pertinent data such as contaminated regions or heat-maps of the injury area were evaluated for the final decision. Extensive testing revealed that using all visual cues improves the efficiency of many baselines, including two of the best network architectures (ResNet50 and DenseNet169) and three other states of the arts from recent

works achieving an accuracy of 89%.

CVR-Net (Coronavirus Recognition Network) is a powerful CNN-based architecture for coronavirus classifications proposed by *Md. Kamrul Hasan* [18]. For the final prediction probability, the outputs of two distinct encoders are mixed. Their proposed CVR-Net has an F1-score and accuracy of 97% and 98%, respectively, compared to existing approaches.

In [19], *Xiang Yu* et al proposed CGNet distinguishing between regular and pneumonia chest X-ray images. On a publicly accessible pneumonia database containing over 5800 X-ray images, their model obtained the highest accuracy of 0.98, the highest sensitivity of 1, and the highest specificity of 0.97. They also put the suggested approach to the test on a publicly accessible CT dataset, with the best results of 0.99% accuracy, 1% specificity, and 0.98% sensitivity, respectively.

Muhammad E. H. Chowdhury in [20] provided a robust approach for diagnosing COVID-19 pneumonia from automated chest X-ray images with the greatest detection accuracy using pre-trained deep-learning algorithms. By combining many public datasets and pulling photos from recently published articles, the scientists created an online database. Using the transfer learning approach and image augmentation, many pre-trained deep Convolutional Neural Networks were trained and validated. The networks were trained to differentiate between two forms of pneumonia: normal and COVID-19 pneumonia, and normal, bacterial, and COVID-19 pneumonia with and without image augmentation. Both methods exhibited classification accuracy of 99.7 percent and 97.9 percent, respectively.

Michael J. Horry et al [21] demonstrate that the VGG19 architecture may be used to build suitable deep learning-based COVID-19 detection tools. The algorithm will classify Pneumonia versus Healthy & COVID-19 vs Pneumonia scenarios for X-ray, ultrasound, and CT scan images. The chosen VGG19 model performs well in COVID-19 identification with up to 86% for X-rays, 100% for ultrasounds, and 84% for CT scans.

Siti Raihanah Abdani et al in [22] proposed a simple DL framework called SPP-COVID-Net for correctly screening the probability of coronavirus. The proposed framework uses a modified spatial pyramid pooling module and 14 layers of convolutional neural networks. The suggested SPP-COVID-Net achieves the highest mean accuracy of 94%

with the lowest standard deviation among the training folds accuracy, according to the output data. The model is well-suited to be used for rapid screening in order to perform better-targeted diagnoses and reduce test time and expense.

Research in [23] uses an X-ray image to train a CNN model to identify and predict a patient's unaffected and impacted illness states. The researchers utilized a dataset of 20k images to test the CNN model's accuracy. The trained-model scored 95% accuracy throughout the success training. Based on the findings of testing, the researchers identified coronavirus on chest X-ray images.

In [24], *Prabira Kumar Sethy* et al developed a deep feature and support vector machine based technique for detecting coronavirus with the assistance of X-ray images. They did this by extracting the deep features of 13 pre-trained CNN frameworks and feeding them to the SVM classifier one by one. In comparison to the other 12 classification models, the ResNet50 + SVM classification model performs well. The proposed classification model for COVID-19 identification has a 95.33% accuracy rate. The accuracy of 95.33% is based on the average of 20 independent executions, with a maximum value of 98.6%.

COVID-Net, a publicly accessible deep convolutional neural network architecture tailored for the identification of COVID-19 cases from chest X-ray (CXR) images was introduced in [25]. They also introduced COVIDx, a benchmark dataset made up of 13k CXR images from 13k patient cases. The framework was able to achieve a highest accuracy of 94% with VGG-19 and Resnet-50 in comparison.

A comprehensive comparison of the research conducted for Covid-19 classification over the years outlining the dataset, year, technique and results is presented in the table 3.1.

3.2 Deep learning segmentation research on COVID-19

In the healthcare sector, image segmentation is still widely used for medical imaging research. It is used in the diagnosis of multiple illnesses for deep learning to figure out the region of interest by computer vision and forecast future consequences, allowing physicians to make quicker care decisions. Several experiments were performed in order to develop an automatic COVID-19 segmentation process. The biggest obstacle though is obtaining the dataset for segmentation. Researchers in this area have done excellent work which is briefly explained in this section.

Table 3.1: Literature Review on Classification

Author	Year	Dataset	Techniques	Results "Accuracy"
Tuan D. Pham	2020	COVID CT Dataset	16 pre-trained Convolutional Neural Netowrk	93% with data augmentation 96% without data augmentation
Tulin Ozturk	2020	Local COVID-19 X-ray Dataset	Darknet Classifier	98 % binary class 87% multi-class
Asif Iqbal Khan	2020	Local COVID-19 X-ray dataset	Coronet Classifier	90% 4-class 95% 3-class 99% binary class
Tanvir Mahmud	2020	Local COVID-19 X-ray dataset	Covxnet CLassifier	97% COVID vs Normal 87% COVID vs Viral Pneumonia 94% COVID vs Bacterial Pneumonia 89% COVID vs Bacterial vs Viral 90% COVID vs Normal vs Bacterial vs Viral
Alejandro	2020	Local COVID-19 CT Dataset	MSTL	89%
Hammam Alshazly	2021	SARS COV 2 CT Dataset COVID CT Dataset	Deep learning based methods	99% 92%
Bin Liu	2020	Local COVID-19 CT Dataset	Lesion-attention deep neural network (LA-DNN)	89%
D. M. H. Nguyen	2020	Local COVID-19 CT Dataset	Deep Learning Models	89%
Md. Kamrul Hasan	2020	3 Local Datasets	CVR-Net (Coronavirus Recognition Network)	91%
Xiang Yu	2021	Local COVID-19 X-ray Dataset	CGNet	99%
Muhammad E. H. Chowdhury	2020	Local COVID-19 Xray Dataset	Pre-trained deep Convolutional Neural Networks	99% with data augmentation 97% without data augmentation
Michael J. Horry	2020	Local COVID-19 CT, X-ray and Ultrasound Dataset	VGG-19	86% X-ray 100% Ultrasound 84 % CT
Siti Raihanah Abdani	2020	Local COVID-19 Dataset	SPP-COVID-Net	94%
Sammy V	2020	Local COVID-19 X-ray Dataset	CNN Model	95%
S.Prabira Kumar Sethy	2020	Local COVID-19 X-ray Dataset	Deep Features and SVM	95%
Linda Wang	2020	Local COVID-19 X-ray Dataset	COVID-Net	94%

A framework called TV-Unet for diagnosing COVID-19 infected chest areas in CT scans was proposed by *Narges Saeedizadeh* [26]. They trained it to recognize ground glass areas at the pixel level. Their experimental study which included everything from visual evaluation of predicted segmentation outcomes to quantitative assessment of segmentation performance revealed that they were able to accurately identify COVID19-associated lung areas with a mIoU rating of over 99% and a Dice score of about 86%.

Adnan Saood in [27] proposed two deep learning networks "U-Net & SegNet" for the coronavirus lung CT image segmentation. Both networks were used as multi-class segmentors as well as binary segmentors. Seventy-two data images were used to train each network and validated on ten images before testing on the remaining eighteen images. The results show that SegNet outperforms the other methods in classifying infected/non-infected tissues with 95% accuracy, while the U-NET outperforms the others as a multi-class segmentor with 91% accuracy.

Instead of using modern or computationally complex neural network architectures, *Dominik Müller* in [28] used a traditional 3D U-Net architecture. By constructing a highly accurate and stable segmentation model for lungs and COVID-19 infected regions, researcher used a 5-fold cross-validation on 20 CT scans of COVID-19 patients without overfitting on the small data. The proposed framework achieved a dice score of 95% for lungs and 76% for infection. They reported that the devised system outperforms competing algorithms, advances the state-of-the-art in COVID-19 segmentation, and improves medical image analysis with less data.

In [29], *A. Amyar* presented a multitask deep learning model to concurrently diagnose COVID-19 patients and segment COVID-19 lesions from chest CT images. A dataset of 1044 patients was utilized to analyze and compare the proposed model with existing image segmentation and classification approaches, comprising 449 patients with COVID-19, 100 healthy patients, 98 patients with lung cancer, and 397 patients with different diseases. The acquired findings show that their system performs brilliantly, with a dice coefficient of 0.78 percent for segmentation and a classification area under the ROC curve of more than 93 percent.

In [30], *Athanasios Voulodimos* examined the effectiveness of deep learning models for semantic segmentation of pneumonia polluted regions in CT images for COVID-19 detection. They tested the efficacy of U-Nets and Fully Convolutional Networks using

real-world CT data from COVID-19 patients. Despite the dataset's class imbalance and man-made annotation errors, the results show that Fully Convolutional Networks can accurately segment and they might also be a potential tool for further research into COVID-19-induced pneumonia symptoms in CT imaging.

In [31], *Kai Gao* et al developed a dual-branch combination network (DCN) for COVID-19 diagnosis accomplishing classification and segmentation of lesion at the same time in their study. To incorporate the intermediate segmentation findings and focus the classification branch more aggressively on the lesion locations, a novel lesion attention module was designed. In their study, they employed a large dataset of 1,202 patients from eleven Chinese institutes. The suggested DCN outperformed other models, achieving an accuracy of 96.74 percent on the internal database and 92.87 percent on the external test datasets.

According to *Kai Gao* et al, their research used a dual-branch combination network (DCN) for COVID-19 detection [31]. Lesion attention modules were meant to include intermediate segmentation data and target the classification branch more aggressively on lesion spots. Using data from 11 Chinese institutions, they studied 1,202 cases. An internal database of 96% and external test datasets of 92% were achieved by the recommended DCN above other models.

In [32], MiniSeg, a lightweight DL framework for effective coronavirus lesion segmentation was proposed. MiniSeg has many important advantages over conventional segmentation methods: i) It only has 83K parameters, making it difficult to over fit; ii) it has a high numerical reliability, making it suitable for realistic deployment. Furthermore, they establish a COVID-19 segmentation benchmark to compare MiniSeg to conventional approaches. The model received an 85% IOU ranking.

In [33], the ADID-UNET is a recently suggested COVID-19 infection segmentation depth network proposed by *Alex Noel Joseph Raj*. To enhance feature propagation and solve the gradient vanishing problem, the framework substitutes convolution and the maximum pooling function. Including an attention gate in the model decreases background noise and improves prediction accuracy. The experimental results demonstrated that the ADID-UNET model can segment COVID-19 lung infected areas with a Dice Coefficient greater than 80%. Furthermore, when compared to other cutting-edge architectures, the suggested model had good segmentation results, earning 80% and 82% on the DC

and F1 scores, respectively.

Tongxue Zhou presented an automatic COVID-19 CT segmentation network based on spatial and channel attention [34]. They recommended a U-Net architecture with a spatial and channel attention structure that re-weights feature representation regionally and channel-wise to catch context - rich interactions for increased feature representation. The studies' results show that the suggested approach can properly and quickly segment COVID-19 data. With this tool, one can segment a CT slices in 0.29 second. The Dice Score, Sensitivity, and Specificity were 83%, 86%, and 99%.

In [35], *Omar Elharrouss* et al suggested an encoder-decoder network-based segmentation system. Computer vision techniques were employed to distinguish the polluted areas of the lungs. The experimental results show accurate segmentation of the lung infection region including both single and multi segmentation when compared to the state-of-the-art methodology. The model received an overall F1-score of 78% for binary segmentation and 64% for multi segmentation.

Yu-Huan Wu developed a novel Joint Classification and Segmentation method for real-time COVID-19 chest CT diagnosis [36]. Tests show the proposed JCS detection method can categorize and segment COVID-19 pretty well. The COVID-CS dataset's classification test set has an average sensitivity of 95%, specificity of 93%, and Dice score of 78%.

The table 3.2 provides an overview of the research conducted on Covid-19 segmentation throughout the years, including the dataset, year, method, and outcomes.

3.3 Research Gaps

Some of the research gaps in the existing literature are summarized below:

- The initial stage in building any diagnostic/prognostic tool is gathering data. That is why the most difficult challenge for the researchers was obtaining the dataset.
- Many researchers used a proprietary dataset, making it impossible to do additional analysis.
- Although vast public databases of more common chest X-rays and CT scans exist, there is no such database of COVID-19 chest X-rays or CT scans optimized for

computational research.

- No previous studies have been found for comprehensive experiments and comparisons with other state of the art architectures for COVID-19 image classification to assist the cad systems.
- There have been no previous research discovered for a detailed experimental study on COVID-19 lesion segmentation on CT benchmark dataset.

Table 3.2: Literature Review on Segmentation

Author	**Year**	**Dataset**	**Technique**	**Results**
Narges Saeedizadeh	2021	Local COVID-19 Dataset	TV-Unet	IOU = 99% Dice Score = 86%
Adnan Saood	2021	Local COVID-19 Dataset	U-Net & SegNet	Acc = 95% "Binary class Segmentation" Acc = 91% "Multi-class Swgmentation"
Dominik Müller	2020	COVID-19 CT Lung and Infection Segmentation Dataset	3D-Unet	Dice Score = 95% "Lungs" Dice Score = 76% "COVID-19 Infection"
A. Amyar	2020	Local COVID-19 Dataset	Multitask Deep learning model of classification & segmentation	Dice Score = 78% ROC = 93%
Athanasios Voulodimos	2020	Local COVID-19 Dataset	U-Net & FCN "Fully Convolutional Neural Network"	F1-Score = 55% "U-net" F1-Score = 65% "FCN"
Kai Gao	2021	Board CT Dataset acquired from 10 Chinese Institutes	Dual Branch Combination Network	Acc = 92%
Yu Qiu	2021	Local COVID-19 Dataset	Miniseg	IOU Score = 85%
YuAlex Noel Joseph Raj	2021	Local COVID-19 Dataset	Attention Gate-Dense Network-Improved Dilation Convolution-UNET "ADID U-Net"	Dice Score = 80% F1-Score = 81%
Tongxue Zhou	2020	Local COVID-19 Dataset	Automatic COVID-19 CT segmentation network using spatial and channel attention mechanism	Dice Score = 83%
Omar Elharrouss	2020	Local COVID-19 Dataset	Encoder Decoder Network	F1-Score = 78% "Binary class Segmentation" F1-Score = 64% "Multi-class Segmentation"
Yu-Huan Wu	2021	Private Dataset	Joint Classification & Segmentation "JCS"	Dice Score = 78%

Chapter 4

Deep Learning

In recent years, deep learning (DL) and machine learning (ML) frameworks have been considered as the "Gold Standard" in computing. There are numerous dynamic cognitive tasks that may be combined or eliminated entirely by using statistical methods, which have become more popular in the area of machine learning and deep learning. With deep learning, one can learn from a large quantity of data. A broad range of traditional applications and fields, like cryptography, natural language processing, bioinformatics, robotics and control, and the analysis of medical data, have all benefited from the fast advancement of deep learning.

As a consequence, this section will provide a general overview of deep learning techniques. A brief introduction to deep learning is followed by a discussion of the differences between deep learning and machine learning, which is followed by a conclusion. Then we explain the situations in which deep learning is required, as well as why we are using deep learning.

4.1 Background of Deep Learning

Deep learning is a subclass of machine learning (Fig: 4.1 [37]) influenced by the human brain's information processing patterns. Observations of data processing patterns in the human brain serve as inspiration for Deep Learning. It does not need any algorithms created by humans in order to function. As an alternative, it makes use of a large amount of data to map the supplied input to specific labels, which saves time. DL is comprised of a number of layers of techniques, each of which provides a unique interpretation of

the information that is provided to it [38, 39].

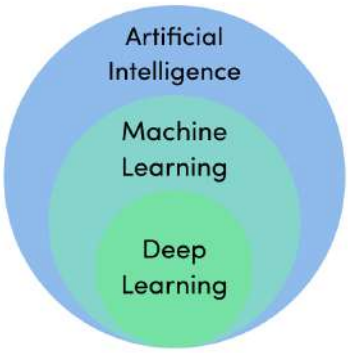

Figure 4.1: Deep Learning Family

Deep learning algorithms, in contrast to typical machine learning approaches, may automate the learning of feature sets for a number of applications [38, 40]. Because of the significant growth and success made in the area of big data in recent years, it's become an enormously popular kind of machine learning approach in the last few years [41, 42]. Its distinguishing performance for various machine-learning tasks is constantly being improved, and it has supported the development of numerous learning disciplines, including image super-resolution, object identification, and image recognition, among others. Recently, deep learning performance has outperformed human performance in domains like as image segmentation and classification, among other applications.

In the year 2020, DL has performed a significant and crucial part in the early diagnosis of a novel coronavirus, which has been identified [43–46]. It has benefited and has become the primary strategy in many hospitals across the globe for the autonomously Covid-19 classification and segmentation using chest X-rays, CT scans, and other forms of imaging, as well as other types of imaging. This section will be concluded with a remark by AI pioneer Geoffrey Hinton, who said that **"Deep learning will be capable of achieving everything"**.

4.1.1 When to apply DL:

Machine learning is useful in many situations, and in certain cases, it is as good as or better than human specialists, implying that deep learning might be a solution in situations when human experts are unavailable or situations in which humans are unable to explain judgments taken in the course of their expertise. Deep learning, in contrast

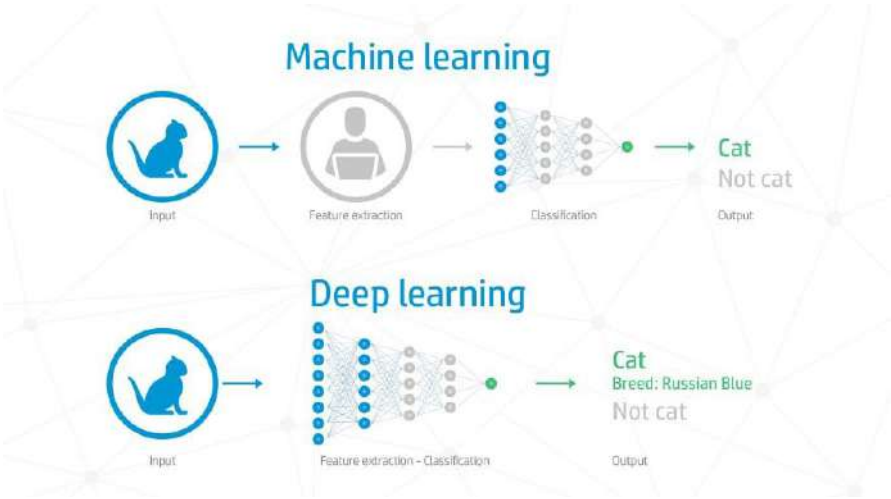

Figure 4.2: Machine Learning vs Deep Learning

to standard machine learning approaches, has the capability of automating the learning of feature sets for a variety of applications. Learning and classification may be accomplished in a single shot thanks to DL technologies (Fig: 4.2 [47]). Furthermore, DL can be a solution to a problem where the solution to the problem changes over time, or where the solution requires adaption based on individual situations.

4.1.2 Why Deep Learning:

Deep Learning techniques outperform conventional approaches when there is a scarcity of domain knowledge for feature introspection because they need less attention to detail in the feature engineering process. Deep Learning is very good at complex tasks such as image classification, natural language processing, and voice synthesis, to name a few examples. The answer to this issue may be found in a variety of performance indicators such as "universal learning method," "robustness," "generalization," and "scalability".

4.1.3 Classification of Deep Learning approaches:

There are three types of DL techniques: unsupervised, partly supervised (semi-supervised) and supervised. Supervised approaches are the most common. Deep reinforcement learning (DRL), sometimes known as reinforcement learning (RL), is a sort of learning approach that is often classified as partly supervised (and occasionally unsupervised) learning.

4.1.4 Types of Deep Learning networks:

Deep learning networks such as recursive neural networks (RvNNs), recurrent neural networks (RNNs), and convolutional neural networks (CNNs) are among the most often used and because of its importance, they are thoroughly described in the next section. Aside from that, it's also the most widely used network across a wide range of applications.

4.2 Convolutional Neural Network

The CNN algorithms are the most well-known and widely used algorithms in the field of deep learning [48]. Compared to its predecessors, CNN has a greater effect and benefit since it can automatically discover critical characteristics without the need for human contact. Convolutional neural networks (CNNs) are extensively employed in a range of fields such as computer vision, voice processing, facial recognition and other similar applications. CNNs, like conventional neural networks, are inspired by neurons found in the brains of humans and animals, as were traditional neural networks.

One version of CNN, which is equivalent to multi-layer perceptron (MLP), comprises of several convolution layers that are followed by sub-sampling (pooling) levels and FC layers near the end of the network. The Framework for image classification is shown in Figure 4.3 [49].

4.2.1 The advantages of using CNN:

The weight sharing characteristic of CNN is the fundamental reason for considering it. It reduces the number of trainable network parameters, enabling the network to increase generalization while avoiding overfitting. Furthermore, as compared to other neural networks, CNN makes the implementation of large-scale networks far simpler.

4.2.2 CNN Layers:

The Framework is composed of numerous tiers that are interconnected. Every layer of a CNN architecture, as well as its function, is discussed in further depth below:

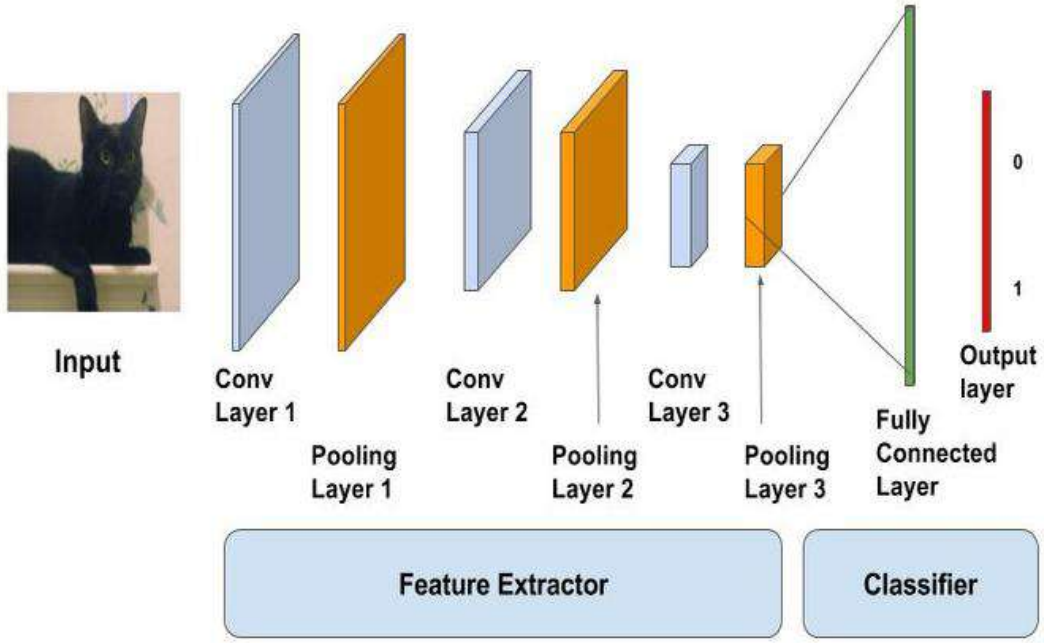

Figure 4.3: CNN Architecture for Image Classification

Convolutional Layer: Filters are applied to source images or feature maps via convolutional layers, which are deep layers. Specified parameters are kept in this location for easy retrieval by the network. The number of kernels and their form are the most key attributes.Figure 4.4 represent an example of the graphical representation of an image and the convolved features for convolution layer [50].

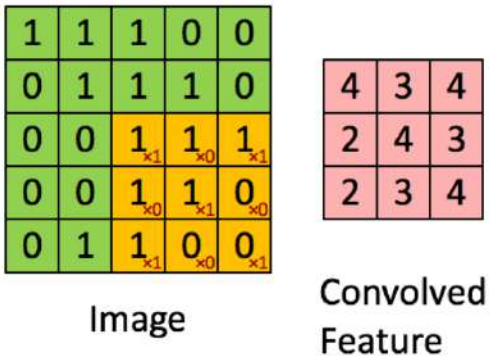

Figure 4.4: Convolutional Layer

Pooling Layer: CNN's are also equipped with pooling layers. For example, it aims to minimise the spatial dimension of a representation progressively, thereby reducing the number of parameters and computation in the network. When it comes to pooling,

the most prevalent option is max pooling. Figure 4.5 [51] shows an illustration of the pooling layer.

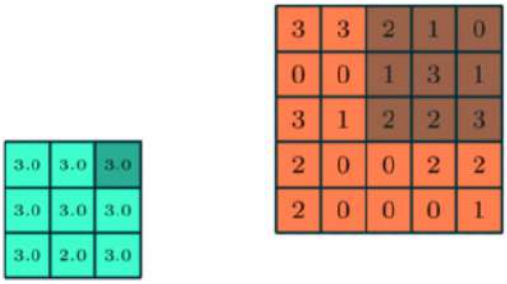

Figure 4.5: Pooling Layer

Activation Function: In neural networks, an activation function is a component that is positioned at the ending of or between two neural networks. They contribute to the determination of whether or not a neuron may fire. The adjusted output is then sent back into the network as input for the next phase of neurons to process. "Sigmoid, Tanh, ReLU, and Leaky ReLU" are the most common types of activation functions used in CNNs as well as other deep neural networks, according to the literature.

Fully Connected Layer: Fully Connected Layers are basically feed forward neural networks in their basic structure and operation. The Fully Connected Levels are the last few layers of the network. The output of the previous Pooling or Convolutional Layer is used as the feed to the fully connected layer, which is flattened and then fed into the fully connected layer as the last step as illustrated in figure 4.6 [52].

Loss Function: Different types of loss functions are used in the CNN output layer to calculate the predicted error that will be created throughout the whole training data set. This error reflects a difference between the intended and actual output. Among the many different types of loss functions that are employed in many problem areas are the Soft max loss function, Euclidean loss function, and Hinge Loss Function.

Regularization: Regularization is one method for preventing overfitting & for controlling model complexity. If there are a lot of features, there will be a lot of weights,

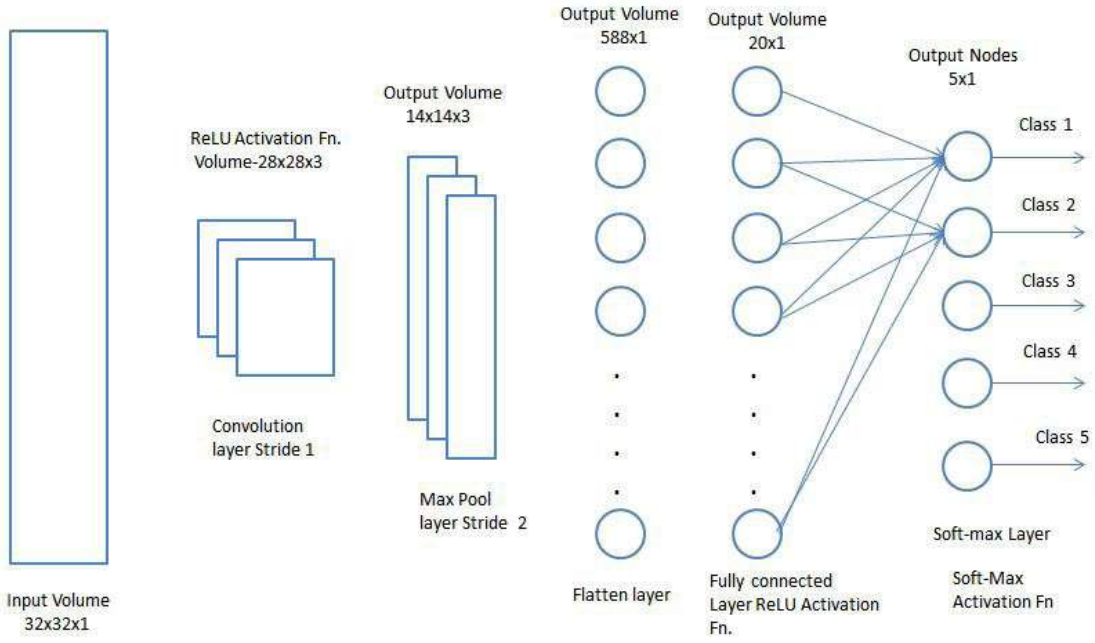

Figure 4.6: Fully Connected Layer

making the model prone to overfitting. As a result, regularisation lessens the strain on these weights. To minimise over-fitting, several intuitive ideas including as dropout, drop weights, batch normalization, data augmentation, and so on are employed to aid regularization.

Optimizer Selection: Optimization techniques or tactics are tactics or methods that are used to alter the properties of a neural network, like as weights and LR, in order to minimise the loss. Optimizer assist in attaining results in a shorter amount of time. Batch gradient descent, adagrad, adadelta, Adam, and other optimization techniques are examples of optimizers that are employed in CNN.

4.3 CNN Architectures

Many CNN architectures have been established in the last decade. CNN's design has undergone several revisions since its inception in 1989. Modifications such as structural reformulation, regularisation, parameter optimization, and so on are examples of this kind of modification. One of the most significant developments in CNN designs has been the use of network depth, which has been the subject of several recent advancements. Throughout this part, we will examine some of the most often used CNN frameworks

for classification and segmentation. Figure 4.7 [53] depicts an example of the layered architecture of a simple convolutional neural network in operation.

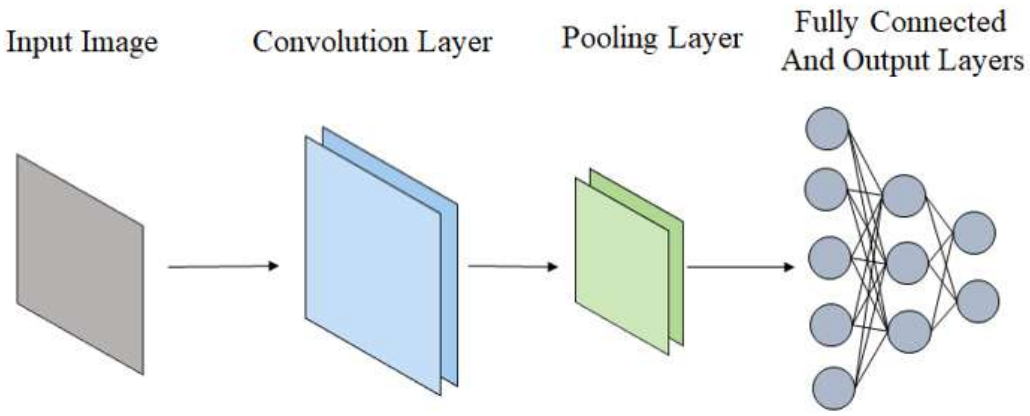

Figure 4.7: An example of layered architecture of a basic convolutional neural network

4.3.1 CNN Architectures for Classification:

VGG Net: It was Simonyan and Zisserman that suggested the VGG network architecture (Fig: 4.8 [54]) , which was presented in their article Very Deep Convolutional Networks for Large Scale Image Recognition, which was published in 2014 [55]. This network is differentiated by its minimalism, since it consists of just three 3x3 convolutional layers that are layered on top of one another in increasing depth. When it comes to volume size reduction, Max pooling is responsible. Following that, two fully-connected layers comprising 4,096 nodes are each followed by a soft max classifier.

Densenet: Dense Net is a recent neural network success in object recognition. Using Dense Net, the output of the preceding layer is coupled with that of the next layer. In order to combat the loss of accuracy caused by the high neural networks with declining gradients, Dense Net was presented, following the same direction as Resnet. The information will be lost before it reaches its ultimate destination because of the lengthy transit between the input and output layers. Figure 4.9 [56] shows the architecture of the dense net network.

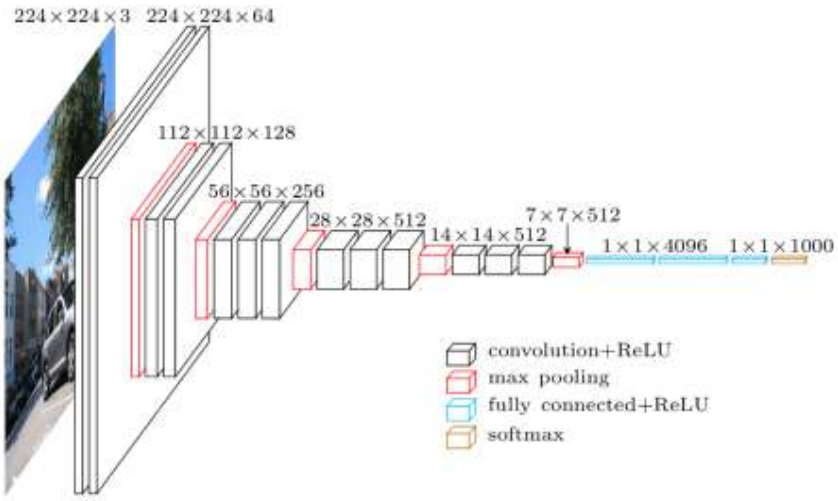

Figure 4.8: VGG architecture

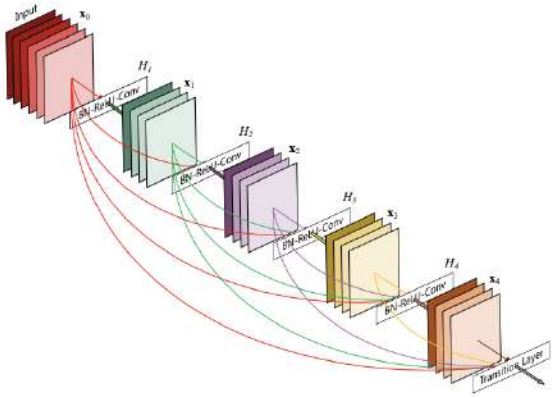

Figure 4.9: The Densenet Architecture

Resnet: As opposed to the more prevalent "VGG," ResNet employs a micro-architecture module known as "network in network," which is more impressive than Alex Net's sequential network design. In this sense, the "micro-architecture" that makes up a network is referred to as "building blocks" as shown in Figure: 4.10 [57]. Resnet is a much more complex network than VGG16 and VGG19, and it was initially reported by He et al. in 2015 [58]. The model's size was drastically lowered by switching from fully-connected layers to average global pooling.

Mobile Net: For usage in portable and embedded vision applications, the convolutional neural network known as MobileNet is designed for this purpose. Because they are built on a reduced architecture, they may develop lightweight deep neural networks with low latency for mobile and embedded devices by using depth wise separable con-

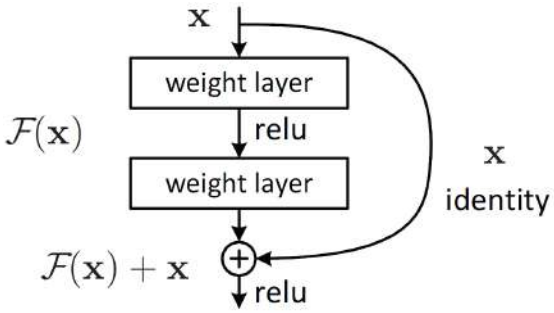

Figure 4.10: Block Diagram of Resnet

volutions. The pixels in the input image are transformed into features that describe the image's content by the MobileNet layers, and these characteristics are then passed on to the other layers. Since it's a feature extractor for another neural network, MobileNet is used in this scenario. The fundamental block diagram for a mobile network is shown in the figure 4.11 [59].

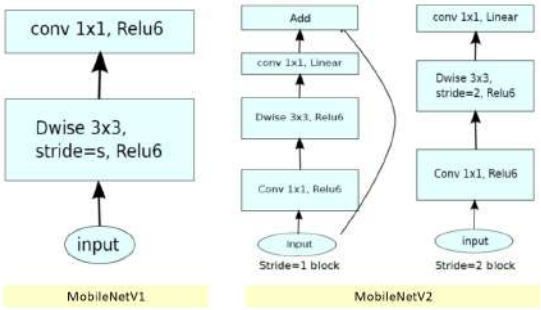

Figure 4.11: Architecture of Mobile net V1 & V2

Xception: François Chollet, the creator and principal developer of the Keras library, came up with the idea for Xception [60]. An architectural update to Inception that substitutes traditional Inception modules with depth-wise separable convolutions is called Xception. Xception networks are shown in the figure 4.12 [61].

Inception(Resnet & V3/4): Inception-ResNet and Inception-V3/4 were proposed by Szegedy et al [62] as upgraded versions of Inception-V1/2. The goal was to lower the cost of computation while increasing network generalisation. Asymmetric small-size filters were chosen over large-size filters by Szegedy and colleagues as a consequence. In addition, they previously employed a bottleneck of 1x1 convolution before utilizing the large-size filters. Traditional convolution is quite similar to cross-channel correlation

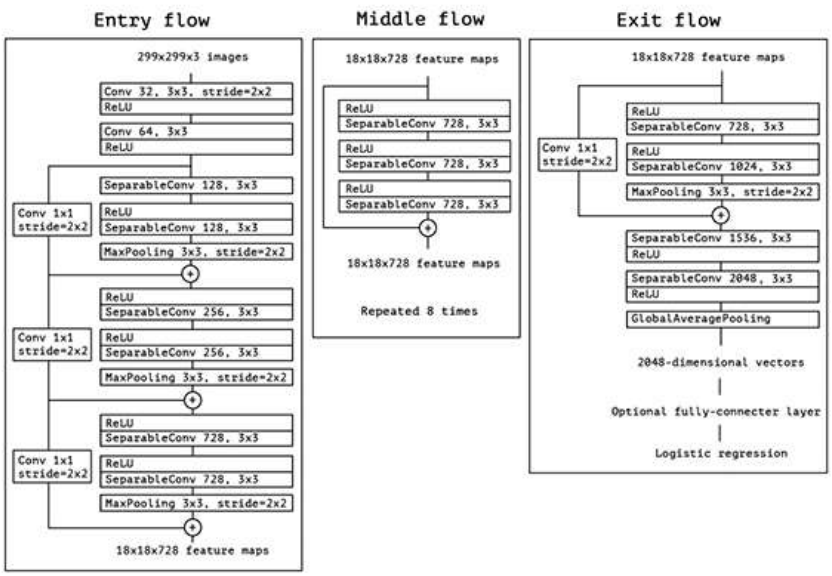

Figure 4.12: The Xception Network

because of these adjustments. Figure 4.13 [63] depicts the fundamental block diagram for the Inception network.

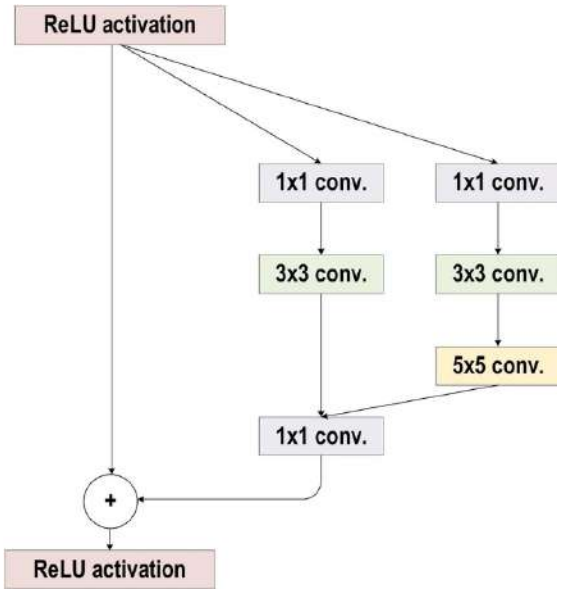

Figure 4.13: The Inception Resnet Architecture

EfficientNet: Using a compound coefficient, EfficientNet is a convolutional neural network design and scaling strategy that equates all depth, breadth, and resolution parameters. Using a compound coefficient, EfficientNet is able to uniformly scale network width, depth, and resolution. The figure 4.14 illustrates the fundamental architecture

of an efficient network [64].

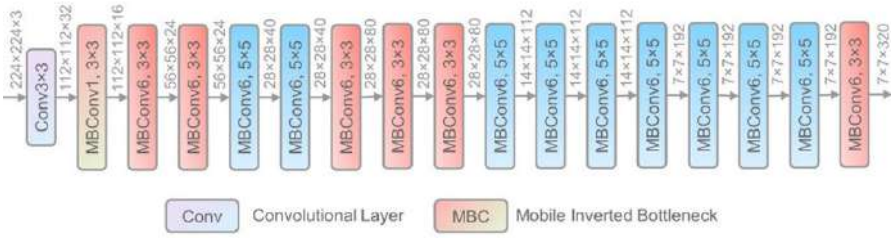

Figure 4.14: The Efficientnet Architecture

Nasnet: In order to find the optimum algorithm for every given task, Nasnet leverages a CNN architecture. It has been shown that networks built using Nasnet outperform those built with hand-coded systems. The search space, the search method, and the performance estimate approach are utilized to classify NAS techniques. The fundamental structure of the Nasnet network is shown in the figure 4.15 [65]

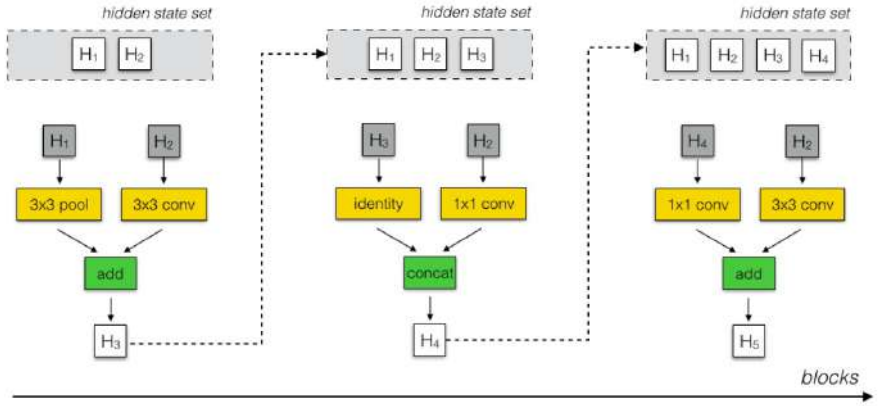

Figure 4.15: Schematic diagram of the NASNet Architecture

4.3.2 CNN Architectures for Segmentation:

Unet: In order to segment biological images, U-Net is a convolutional neural network that has been created specifically for this purpose. U-Net was given its name because its architecture, when visualized, resembled that of the letter U. The architectural design of the system is separated into two parts: the left half, which represents the contracting route, and the right part, which represents the expanding route. In the contracting route, the goal is to capture context, while in the expanding path, the purpose is to assist in correct localization.

Contracting route is composed of two convolutions of three by three. There is a rectified linear unit and a two-by-two max-pooling computations after the convolutions, which is used to down sample the results. The unet's core architecture for image segmentation is shown in figure 4.16 [66].

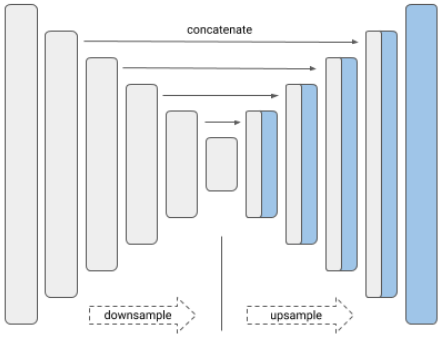

Figure 4.16: The Unet Architecture

Feature Pyramid Network (FPN): Another comparable design is Feature Pyramid Network (FPN), however, instead of copying and attaching features like in Unet, FPN applies a 1x1 convolution layer and adds the features to it. The figure 4.17 demonstrates the FPN's main architecture for image segmentation [66].

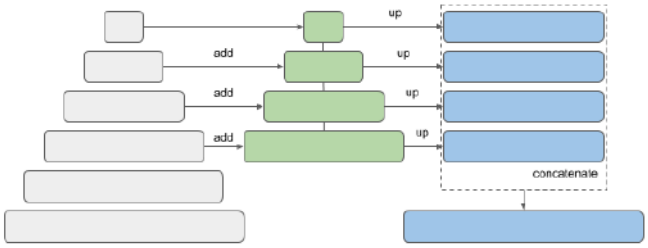

Figure 4.17: The FPN Architecture

Pyramid Scene Parsing Network (PSPNet): PSPNet, or Pyramid Scene Parsing Network, is a semantic segmentation approach that use a pyramid parsing module to

leverage global context information via context aggregation depending on various regions. The combination of local and global cues strengthens the ultimate prediction. Figure 4.18 depicts the pspnet image segmentation architecture [66].

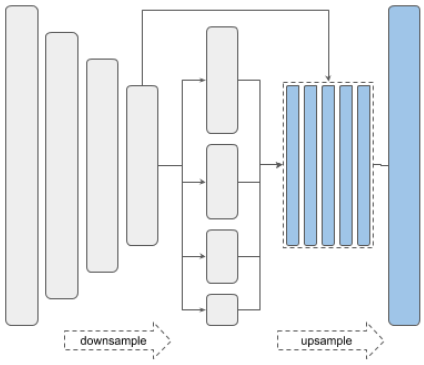

Figure 4.18: The PSPNet Architecture

Link Net: For semantic segmentation, a deep neural network architecture called Linknet was developed. It can provide real-time performance on both GPU's and embedded devices. Members of Purdue University's e-Lab designed this network. Linknet can process an input image with a resolution of 1280x720 at a rate of 2 frames per second and 19 frames per second, respectively. After each down sampling block, the Linknet architecture attempts to efficiently exchange the knowledge learned by the encoder with the decoder. This outperforms utilizing pooling indices in the decoder or simply employing fully convolutional networks in the decoder. This feature forwarding approach not only provides with high accuracy values, but it also allows us to have only a few parameters in our decoder. The figure 4.19 depicts the linknet essential architecture for image segmentation [66].

4.4 Applications of Deep Learning

Deep learning implementations are now being employed all around the globe, and there are several examples of them. Some examples of these applications include health care coverage, social network analysis, sound and voice processing (such as recognition and enrichment), visual information processing techniques (such as audio - visual data processing and computer vision), and natural language processing (such as translation and

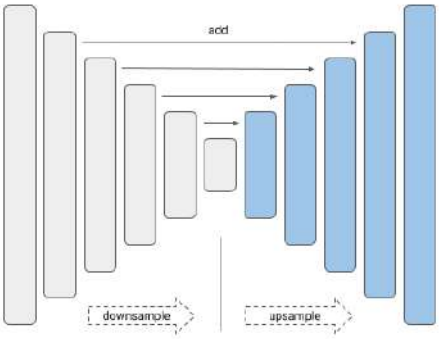

Figure 4.19: The LinkNet Architecture

sentence classification) (Fig 4.20 [67]). These applications may be classified into five categories: classification, localisation, detection, segmentation, and registration, to name a few examples. However, even though they all have different goals, the pipeline implementation of these apps is quite similar.

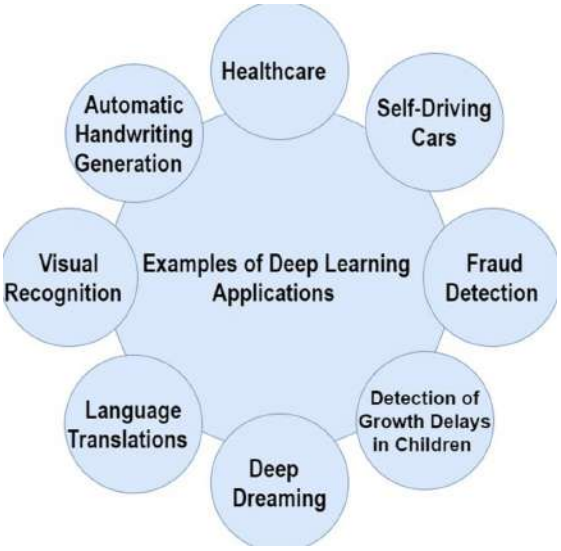

Figure 4.20: Example of DL Applications

Healthcare is one of the most significant and diverse DL applications. Because of its relevance to human lives, this field of study is essential. Furthermore, DL has demonstrated exceptional performance in healthcare.

4.5 Evaluation Metrics

The evaluation metrics that are utilized in deep learning are crucial in achieving the best possible results. Here are among the most widely used assessment measures in use today.

Accuracy: This function computes the proportion of correctly predicted classes to the total number of samples tested.

Recall: Applied to determine the proportion of positive patterns that are accurately categorized.

Precision: This method is used to determine the proportion of negative patterns that are accurately categorized as negative.

F1-Score: This function computes the harmonic average of the recall and precision rates.

Jaccard Index: When comparing two sample sets, the Jaccard index, commonly termed as the Jaccard coefficient, is used to determine how similar and diverse the two sets are.

$$\text{Recall} = \frac{TP}{TP + FN} \tag{4.1}$$

$$\text{Precision} = \frac{TN}{TN + FP} \tag{4.2}$$

$$\text{Accuracy} = \frac{TP + TN}{TP + TN + FP + FN} \tag{4.3}$$

$$\text{Jaccard Index} = \frac{TP}{TP + FP + FN} \tag{4.4}$$

$$\text{F1Score} = \frac{2TP}{2TP + FP + FN} \tag{4.5}$$

4.6 Summary

The ongoing evolution of artificial intelligence offers up new options for machine development. Deep Learning and Machine Learning are both regarded to be subcategories of Artificial Intelligence, although they are not interchangeable. Both Machine Learning and Deep Learning have distinct algorithms that are capable of performing certain tasks, each with its own set of advantages. Machine Learning algorithms are able to evaluate and learn from supplied data, and they are ready to make a final decision with the assistance of a human assistant; however, deep learning algorithms do not necessitate as much support and sustain to fundamental replication of human brain processes and comprehension of the context, as opposed to machine learning algorithms.

According the article, titled **"Deep Learning for AI"** [68] deep learning models will be adaptable to change in their environment and manage a broad variety of cognitive and reflexive challenges in the future.

Chapter 5

Proposed Methodology

In this chapter, the proposed classification and segmentation methodology for the automatic analysis of COVID-19 disease is provided. Moreover, a brief details of the datasets is also being discussed in this chapter. We will begin with the datasets and then to the proposed classification and segmentation techniques.

In addition, certain ideas of transfer learning, implementation, performance evaluation measures, and model hyperparameters for developing classification and segmentation models are discussed.

5.1 Databases

The proposed methodology is evaluated using freely available classification and segmentation datasets plus the table 5.1 and 5.2 reports the total number of images, as well as the URLs for classification and segmentation datasets respectively.

5.1.1 Classification Datasets:

SARS COV II (Kaggle): Eduardo Soares et al created the SARS-CoV-2 CT scan dataset, which comprises 1252 Covid CT scans plus 1229 non-Covid CT scans for patients, totaling 2481 CT scans. These data were gathered from legitimate patients at hospitals in Sao Paulo, Brazil [69]. Figure 5.1 shows sample images of the dataset.

COVID CT (GitHub): Xingyi Yang et al published a CT image database of 349 CT scans of COVID-19 confirmed cases from 216 individuals plus 195 non-COVID-19 CT

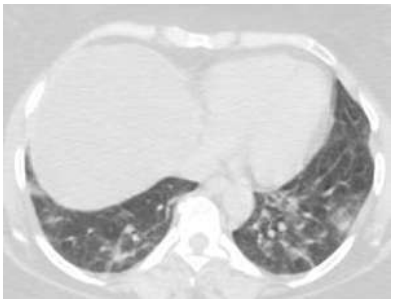

(a) COVID CT Scan

(b) Non-COVID CT Scan

Figure 5.1: CT Scans of SARS COV II Dataset

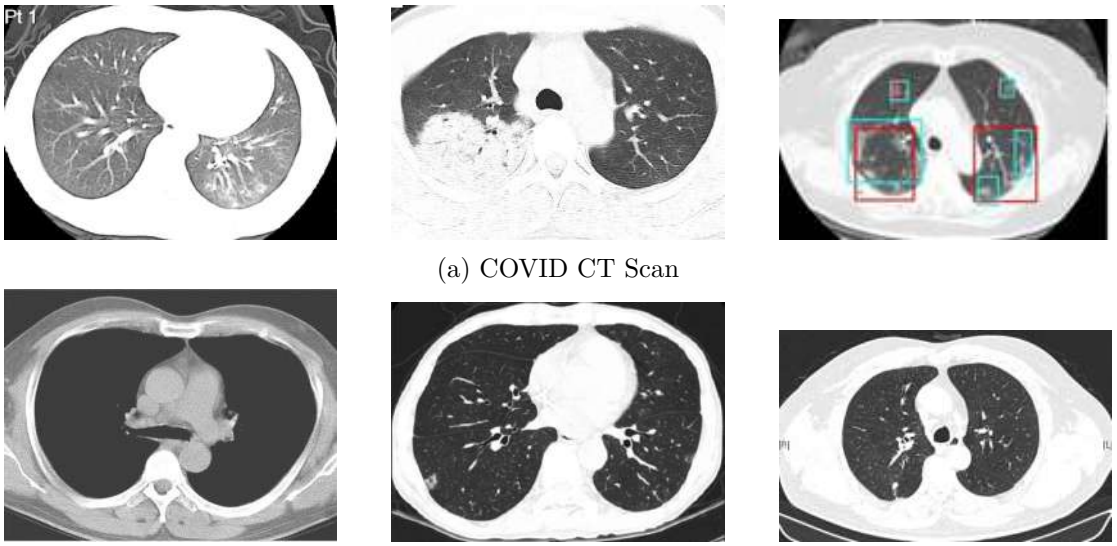

(a) COVID CT Scan

(b) Non-COVID CT Scan

Figure 5.2: CT Scans of COVID CT Dataset

scans [70]. The image 5.2 represents some sample of CT scan images from the dataset, including both COVID and non-COVID scans.

Radiography X-ray Database (Kaggle): A database of chest X-ray images of COVID-19 affirmative patients, normal and viral pneumonia images was established through collaboration with medical physicians, a group of researchers from the University of Dhaka and Qatar University, as well as some other team members from Malaysia and Pakistan. In their current release, there are 3616 COVID-19 positive photos, 10.2k normal views, and 1345 Pneumonia images. They will continuously update this database when additional X-ray images for COVID-19 patients become available [20, 71]. Figure 5.3 depicts some sample images of x-ray scans of COVID, normal, and viral pneumonia from the dataset.

(a) COVID X-ray Scan (b) Normal X-ray Scan (c) Pneumonia X-ray Scan

Figure 5.3: X-ray Scans of COVID Radiography Dataset

Joseph Paul Cohen COVID X-ray Dataset: Joseph Paul Cohen and colleagues published the very first online COVID-19 X-ray image database. This dataset now contains hundreds of frontal view X-rays and is the most comprehensive public asset for COVID-19 imaging plus prognostic data, making it an essential resource for developing and assessing technologies that can aid in COVID-19 diagnosis. In their current release, there are 435 COVID and 505 Non-COVID chest X-ray photos from 412 patients from 26 countries, and this numbers are increasing [72]. In the figure 5.4, COVID vs normal x-ray images from the database are shown.

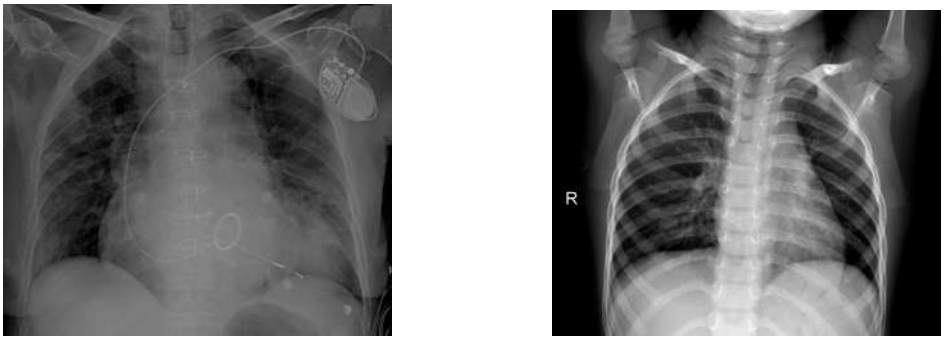

(a) COVID X-ray Scan (b) Non-COVID X-ray Scan

Figure 5.4: X-ray Scans of COVID IEEE-8023 Dataset

Table 5.1: Overview of the Classification Datasets

Classification Method	**Number of Samples**	**Links**
Binary Class	2481 CT Scans	https://www.kaggle.com/plameneduardo/sarscov2-ctscan-dataset [69]
Binary Class	544 CT Scans	https://github.com/UCSD-AI4H/COVID-CT [70]
Binary Class	940 X-ray Scans	https://github.com/ieee8023/covid-chestxray-dataset [72]
Multi Class	15153 X-ray Scans	https://www.kaggle.com/tawsifurrahman/covid19-radiography-database/data [20, 71]

5.1.2 Segmentation Datasets:

Medical Segmentation: This dataset consists of two parts "Radiopedia and MedSeg" [73]. The Medseg section includes 100 axial CT scans from 40 COVID-19 patients that have been converted from publicly available JPG pictures. A radiologist applied three labels to segment the image.: ground-glass, consolidation, lungs. The radiopedia section comprises a dataset with volumes of both positive and negative slices; 373 of a total of 829 slices were rated as positive and segmented by a radiologist. The CT images and masks are shown in figure 5.5.

Ground glass opacity (GGO) refers to the hazy grey regions that may be seen in lungs CT scans or X-rays. The grey patches represent increased density throughout the lungs. Lung consolidation occurs when the air that ordinarily fills the lungs' small airways is supplanted with something else. This air may be filled by a liquids like pus, blood, or water, or a substance like stomach contents or cells, depending on the reason.

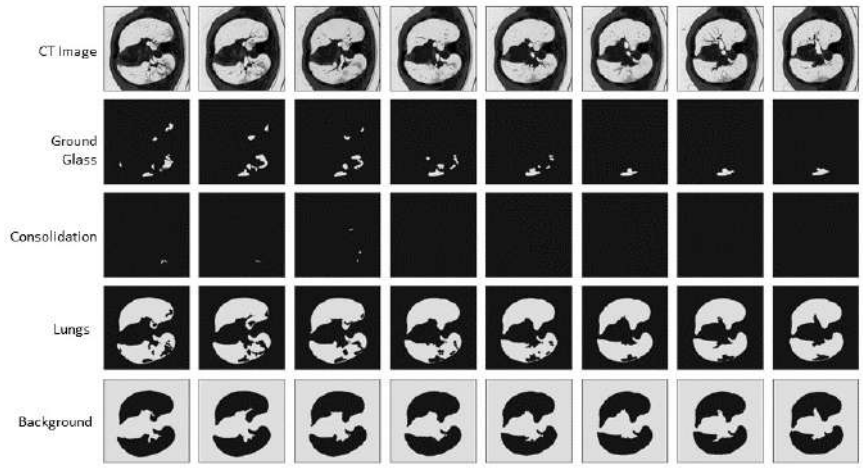

Figure 5.5: Visual Appearance of Medical Segmentation Dataset with Masks

COVID-19 CT Lung & Infection Dataset (Zenodo): The second dataset comprises 20 CT images of COVID-19 patients, as well as expert segment of lungs and infections. A radiologist utilized three labels to segment the images: "Lung mask, Disease mask, Lung + Disease mask." (Fig: 5.6) [74].

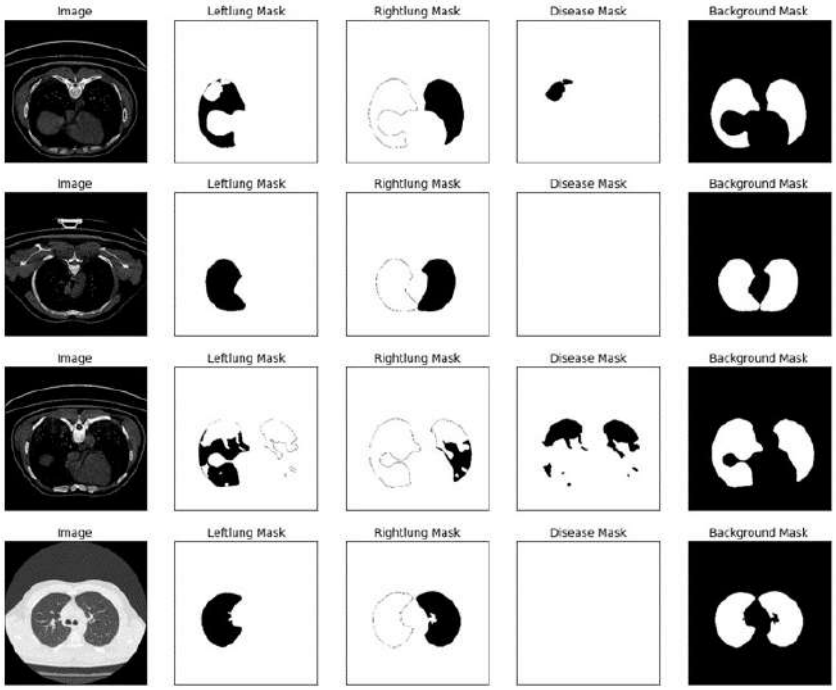

Figure 5.6: Visual Appearance of Zenodo Dataset with Masks

Table 5.2: Overview of the Segmentation Datasets

Segmentation Method	**Number of Samples**	**Links**
Binary & Multi-Class	20 CT Scans	https://zenodo.org/record/3757476#.YUG_UMvivIV [74]
Multi-Class	100 CT Scans from 40 patients	http://medicalsegmentation.com/covid19/ [73]
Multi-Class	829 slices from 9 patients	http://medicalsegmentation.com/covid19/ [73]

5.2 Proposed Architecture for Classification

As discussed earlier, the proposed classification model will segregate COVID-19 CT & X-ray images from healthy images by performing classification.

The CNN architectures used for feature extraction purpose are mentioned below with variants shown in parenthesis and the basic workflow of COVID-19 classification is shown in figure 5.7. Details are discussed in chapter 4.

- VGG (16,19)
- Densenet (121)
- Nasnet (Large)
- Efficientnet (B0)
- Mobilenet (V2)
- Resnet (50, 50V2, 101V2)

- Xception
- Inception (Resnet V2, V3)

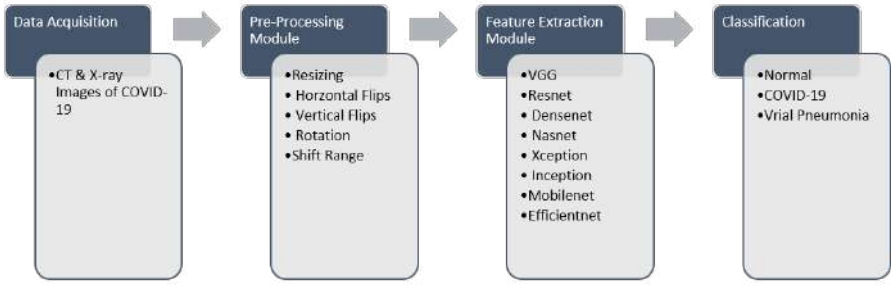

Figure 5.7: Workflow of COVID-19 Classification

5.2.1 Proposed Architecture:

In our investigation, we used deep CNN architectures for binary and multi-class classification, and we used COVID-19 as the target concept in seeing how the classification algorithm predicts COVID-19 cases.

The block diagrams for training & testing of the proposed architecture are shown in figure 5.8 and 5.9 respectively.

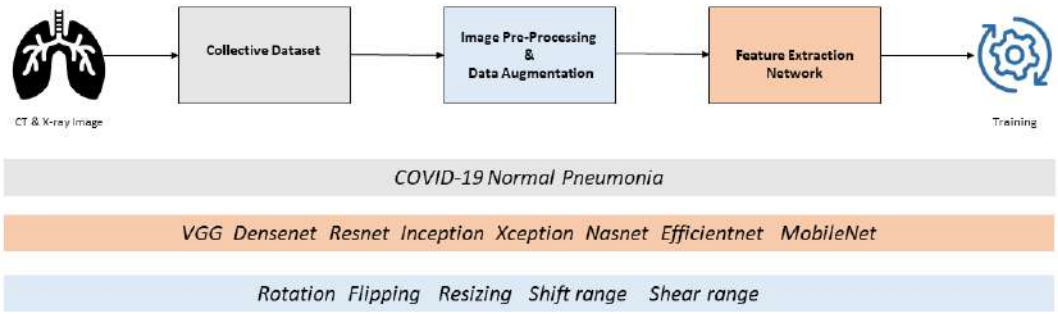

Figure 5.8: Block Diagram for Training

5.2.2 Transfer Learning:

Generally, transfer learning is a machine learning approach in which an existing model that has been previously trained is used as the basis for a newly created model and task.

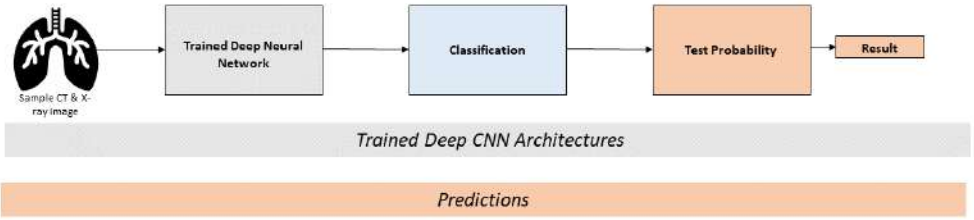

Figure 5.9: Block Diagram for Testing

The amount of work required to obtain training data may be reduced significantly, and the training process can be accelerated as well.

Two strategies are utilised to exploit transfer learning on deep convolutional neural networks. To begin, the pretrained model is used to extract picture features for the new classification model while retaining its original architecture and learned parameters. The second strategy updates the pretrained model's architecture and parameters to enhance retrieved picture features on the fresh dataset.

The first method is employed in this study. Moreover,to pretrain CNN architectures, we leverage ImageNet, a large-scale dataset comprising of 1.2 million high-resolution images in 1,000 distinct classes (e.g., fish, bird, tree, flowers, sport, room, etc.).

5.2.3 Data Augmentation:

In deep learning neural networks, the availability of data regularly improves the performance of the network. In data augmentation, new training data is generated from current training data using a variety of techniques. It refers to the changes in the training set images that the algorithm is likely to take into consideration.

Multiple libraries are available for data augmentation in Python. PIL and Augmentor are two libraries that can operate on images directly. Augmentor also has a pipelining

feature that allows us to work on many images at once. Apart from keras preprocessing, we used ImageDataGenerator. Rotation, cropping, zooming, colour range modifications, grayscaling, and flipping are examples of image augmentations.

Data augmentation can be divided into two groups. The first is image transformation, while the second is the creation of synthetic images. We used transformation data augmentation technique for the classification problem. The techniques for data augmentation used for classification are listed in the table 5.3.

Table 5.3: Data Augmentation for Classification

Augmentation	**Probability**
Rotation	20
Flipping	Horizontal
Resizing	True
Shift Range	0.2
Shear Range	0.2
Zoom Range	0.2

5.2.4 Model Hyperparameters:

The following hyperparameters are used for training:

Binary Classification Model: Image size = 224x224, Batch size = 32, cross entropy loss, Adam optimizer with LR = 0.0001, 20 epochs in total with early stopping.

Multi Classification Model: Image size = 240x240, Batch size = 32, cross entropy loss, Adam optimizer with LR = 0.0001, 50 epochs in total with early stopping.

5.2.5 Evaluation Metrics:

Five major performance metrics are used to assess the suggested model's performance: accuracy, confusion matrix, precision, recall, and F1-score.

Confusion Matrix: For the classification issue, confusion matrix provides a summary of anticipated and true labels. It provides information not just about the mistakes but also on the sorts of errors made by the classifier. Figure 5.10 depicts the confusion matrix schema in a classification problem [75].

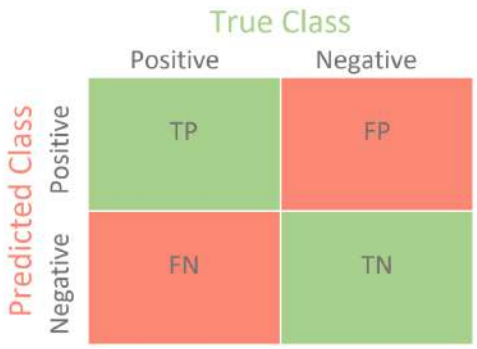

Figure 5.10: Schema of confusion matrix

Based on the confusion matrix, the accuracy, precision, recall, and F1-score can be calculated using the formulas mentioned below:

$$\text{Accuracy} = \frac{TP + TN}{TP + TN + FP + FN} \tag{5.1}$$

$$\text{Precision} = \frac{TN}{TN + FP} \tag{5.2}$$

$$\text{Recall} = \frac{TP}{TP + FN} \tag{5.3}$$

$$\text{F1Score} = \frac{2TP}{2TP + FP + FN} \tag{5.4}$$

5.3 Proposed Architecture for Segmentation

The goal of segmentation is to determine the region of interest from an image. In our situation, the area of the lung affected by the coronavirus and the lungs in CT images.

The architectures used for the COVID-19 semantic segmentation are mentioned below with backbones used along with the workflow of COVID-19 segmentation in figure 5.11.

Architectures:

- Unet

- Link Net
- Pyramid Scene Parsing Network (PSPNet)
- Feature Pyramid Network (FPN)

Backbones

- VGG-19
- Densenet 121
- Seresnext 101
- Inception Resnet V2
- Efficientnet B3
- Mobilenet V2

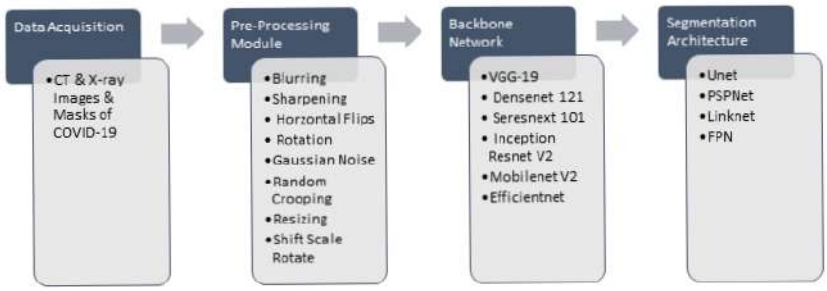

Figure 5.11: Workflow of COVID-19 Segmentation

5.3.1 Proposed Architecture:

Our segmentation problem is a binary & multi-class problem. So we have two classes for binary class & four classes for multi-class. The details of the classes and the masks are shown in the table 5.4.

The block diagram for training & testing of the proposed architecture are shown in Fig 5.12 and 5.13 respectively:

Table 5.4: Segmentation Masks

Class	Segmentation Masks
Binary Class	Disease
	Background
Multi Class	Ground Glass
	Consolidation
	Lungs
	Background
Multi Class	Disease
	Left Lung
	Right Lung
	Background

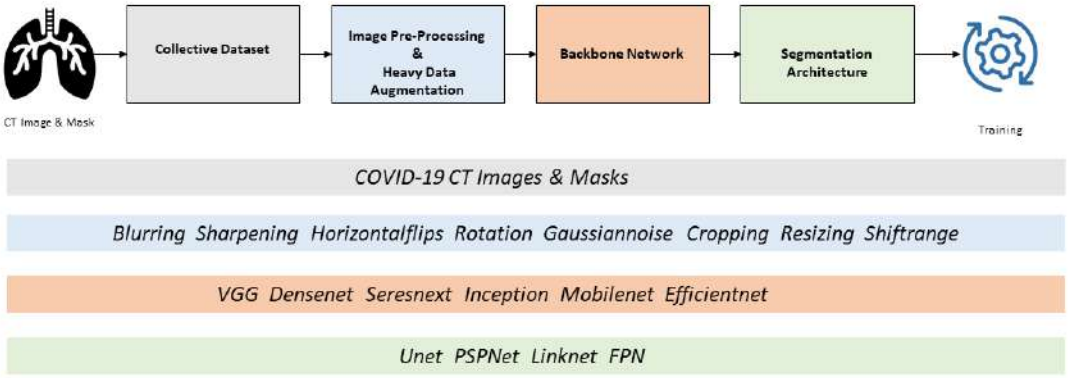

Figure 5.12: Block Diagram for Training

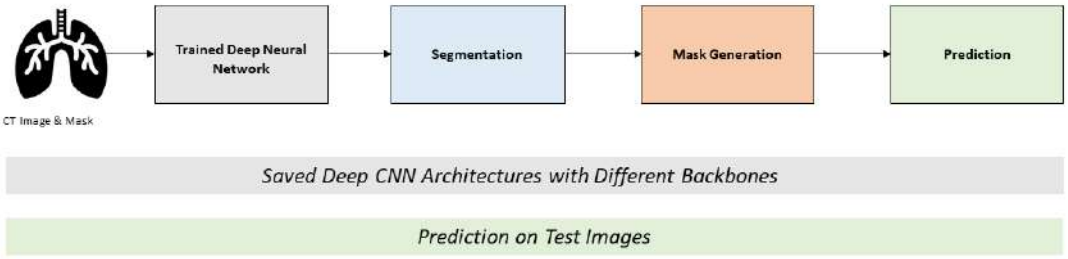

Figure 5.13: Block Diagram for Testing

5.3.2 Data Augmentation:

The availability of annotated training data is frequently a constraint in medical image segmentation. 'Data augmentation' prevents the network from memorising training data and improves its performance on data outside of the training set. As a result, it is critical in the development of effective deep learning pipelines.

Due to limited number of COVID CT segmented image and masks, data augmentation using the synthetic image creation theme was utilized. Using the "albumentation library" on binary & multi-class segmentation, resizing, horizontal flips, shift scale rotate, cropping, Gaussian noise and perspective augmentation have been utilized for best results. Table 5.5 shows the applied augmentation techniques with probabilities.

Table 5.5: Data Augmentation for Segmentation

Augmentation Technique	**Probability**
Random Crop	True
Flipping	Horizontal (0.5)
Resizing	True
Shift	0.1
Scale	0.5
Rotate	0
Gaussian Noise	0.2
Blurring	0.1
Sharpening	0.1

5.3.3 Hyperparameters:

The hyperparameters for segmentation that have been used are shown below:

Binary Class Segmentation: Image size = 320x320, Batch size = 8, dice & focal loss, Adam optimizer with learning rate = 0.0001, 20 epochs in total with early stopping.

Multi-class Segmentation: Image size = 256x256 (Zenodo) and 512x512 (Medical Segmentation), Batch size = 16, total loss which is a combination of weighted binary cross entropy, focal loss and twesvky loss, Adam optimizer with learning rate = 0.0001, 25 epochs in total with early stopping.

5.3.4 Evaluation Metrics:

For the Segmentation problem, Jaccard Index & F1-score are used for evaluation.

$$\text{Jaccard index} = \frac{TP}{TP + FP + FN} \tag{5.5}$$

$$\text{F1Score} = \frac{2TP}{2TP + FP + FN} \tag{5.6}$$

Chapter 6

Experimental Results

6.1 Results

The results of classification and segmentation proposed architectures will be discussed in this section.

6.1.1 Binary Class Classification's Performance:

The binary classifier was implemented on three datasets and consists of two datasets for CT scans & one for X-ray scans namely *"SARS COV II, IEEE-8023, COVID CT DS GitHub"*. Accuracy, precision, recall and F1-score were the evaluation metrics employed. All of the findings have been summarized in Table 6.2.

Train Test Split: The *COVID CT* dataset includes 349 COVID CT scans and 195 healthy CT scans, with 408 utilised for training and 136 for testing. Similarly, the *SARS COV II*CT Dataset includes 1252 COVID images as well as 1229 non-COVID images. 1860 images have been utilized for training, and 621 images have been used for testing, with a train test ratio of 20%.. Finally, the *IEEE 8023* X-ray dataset includes 940 X-ray scans, 435 of which are positive COVID X-rays and 505 of which are healthy X-rays. Using a 20% train-test split, 752 x-rays were utilised for training and 188 for testing. Table 6.1 shows the ratio of the train test split.

Results: On three COVID-19 binary class datasets, we compared the results of 9 deep learning architectures with other state-of-the-art architectures and methods for binary

Table 6.1: Train Test Split for Binary Class Classification

Dataset	Total Number of Images	Training	Testing
SARS COV II	2481	1860	621
COVID CT DS GitHub	544	408	136
IEEE-8023	940	752	188

class classification and the performance of the proposed framework was equated using the accuracy, precision, recall, and F1-Score of the test dataset. A closer inspection of the table 6.2 reveals that DL architectures are reliable for diagnosing COVID-19. Resnet 101 V2 architecture emerges the best with maximal accuracy of 96% and 97% on *"COVID CT DS GitHub & IEEE-8023 X-ray dataset"* while VGG-16 architecture performs best with a maximal accuracy of 98% on *SARS COV II CT dataset.*

The confusion matrices for the binary classification results of all three dataset are shown in Figure 6.1, 6.2 and 6.3.

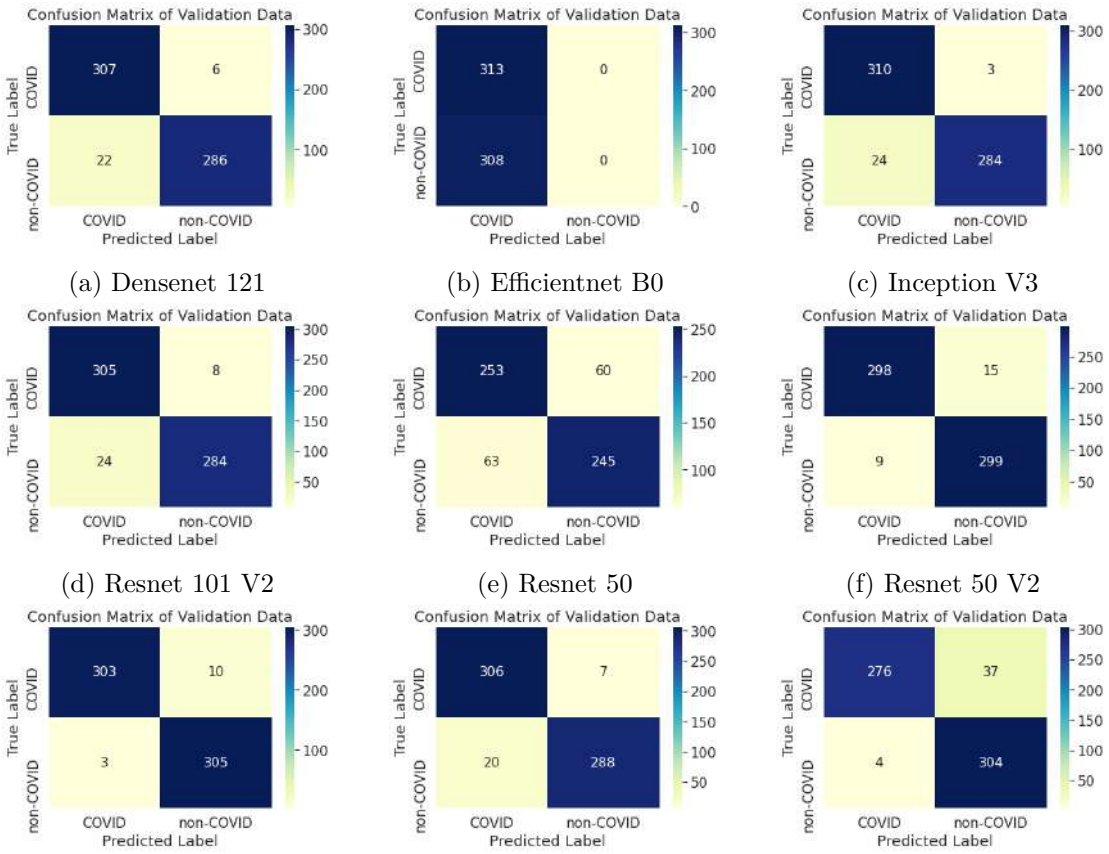

(a) Densenet 121 (b) Efficientnet B0 (c) Inception V3

(d) Resnet 101 V2 (e) Resnet 50 (f) Resnet 50 V2

(g) VGG 16 (h) VGG 19 (i) Xception

Figure 6.1: Confusion Matrix for SARS COV II CT Dataset

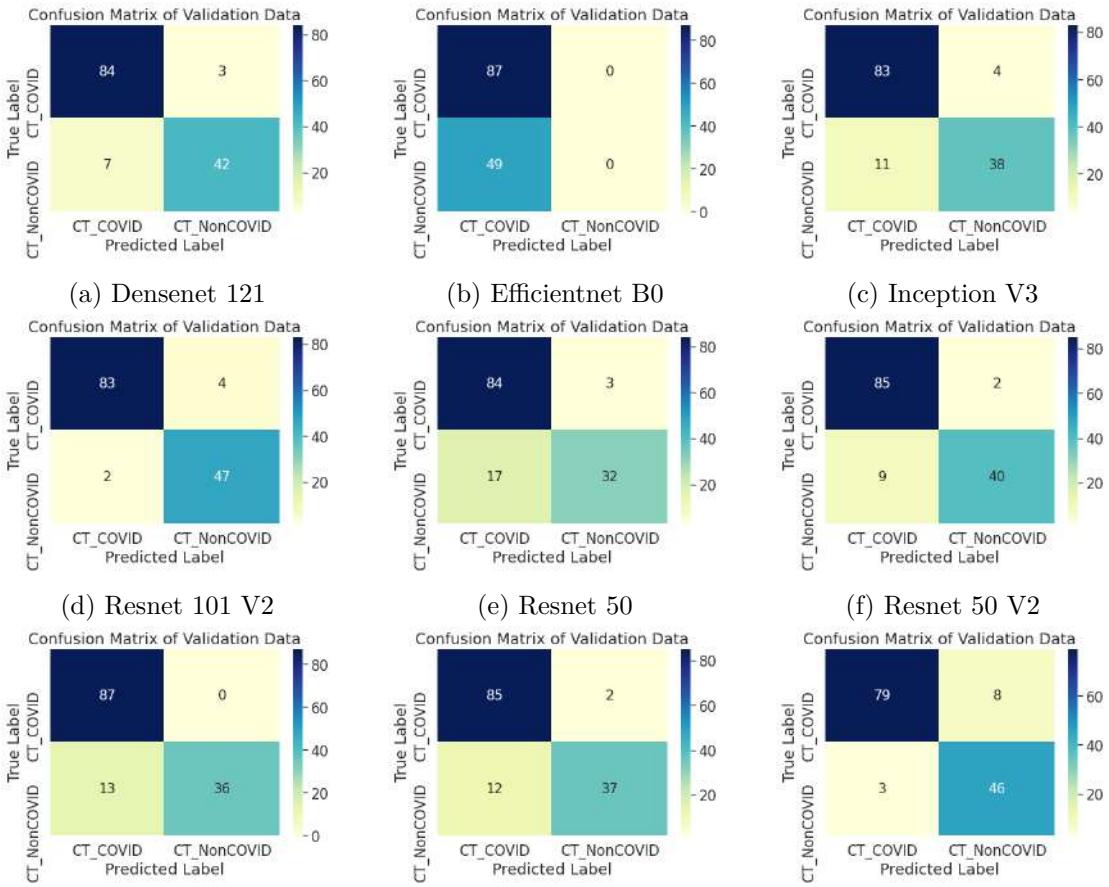

(a) Densenet 121 (b) Efficientnet B0 (c) Inception V3

(d) Resnet 101 V2 (e) Resnet 50 (f) Resnet 50 V2

(g) VGG 16 (h) VGG 19 (i) Xception

Figure 6.2: Confusion Matrix for COVID-CT Dataset

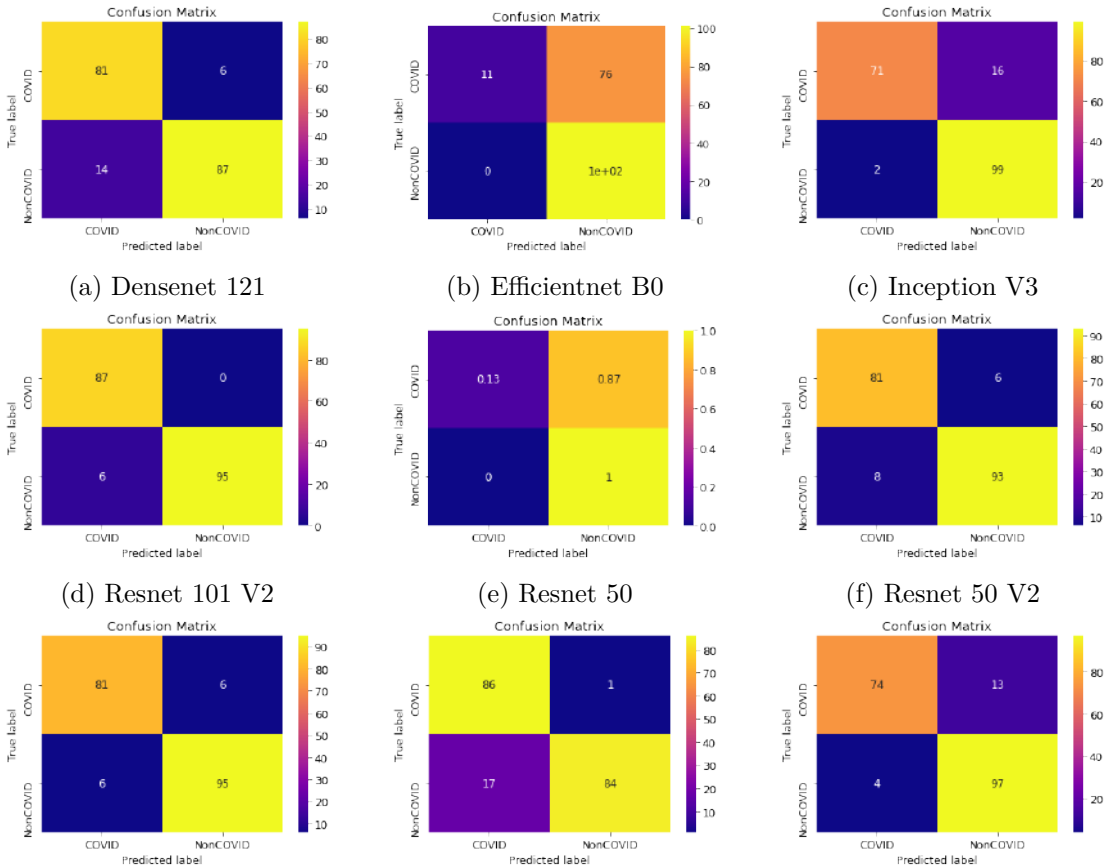

(a) Densenet 121 (b) Efficientnet B0 (c) Inception V3

(d) Resnet 101 V2 (e) Resnet 50 (f) Resnet 50 V2

(g) VGG 16 (h) VGG 19 (i) Xception

Figure 6.3: Confusion Matrix for IEEE 8023 Dataset

Table 6.2: Evaluation Metrics for Binary Classification

Datasets	Model	Accuracy	Precision	Recall	F1-Score
IEEE 8023 *X-ray (Binary class) [72]*	VGG-16	0.94	0.94	0.94	0.94
	VGG-19	0.90	0.91	0.91	0.90
	Xception	0.91	0.92	0.91	0.91
	ResNet 50 V2	0.93	0.92	0.93	0.93
	Inception V3	0.90	0.92	0.90	0.90
	Res Net 101 V2	**0.97**	**0.97**	**0.97**	**0.97**
	Dense Net 121	0.89	0.89	0.90	0.89
	ResNet 50	0.60	0.79	0.56	0.48
	Efficient net B0	0.60	0.79	0.58	0.49
SARS COV II CT Scan DS (Binary class) [69]	Xception	0.93	0.88	0.99	0.93
	Inception V3	0.96	0.99	0.93	0.96
	Dense Net 121	0.95	0.98	0.93	0.96
	VGG-16	**0.98**	**0.97**	**0.99**	**0.98**
	VGG-19	0.96	0.98	0.94	0.96
	ResNet-50	0.80	0.81	0.80	0.80
	Resnet50v2	0.96	0.95	0.97	0.96
	Resnet101v2	0.95	0.97	0.93	0.95
	Efficientnet B0	0.50	1.00	0.50	0.67
COVID CT DS GitHub (Binary class) [70]	VGG-16	0.90	1.00	0.87	0.93
	VGG-19	0.90	0.98	0.88	0.92
	Xception	0.92	0.85	0.96	0.90
	ResNet 50 V2	0.92	0.98	0.90	0.94
	Inception V3	0.89	0.95	0.88	0.92
	Res Net 101 V2	**0.96**	**0.95**	**0.98**	**0.97**
	Dense Net 121	0.93	0.97	0.92	0.94
	Efficient Net B0	0.64	1.00	0.64	0.78
	ResNet 50	0.85	0.97	0.83	0.89

6.1.2 Multi Class Classification's Performance:

The COVID-19 radiography X-ray database was used to implement the multi class classification, which comprises chest X-ray images of normal, viral pneumonia, and COVID-19 positive patients.. The evaluation methods used were accuracy, precision, recall and F1-score. Table 6.4 summarises all findings.

Train Test Split: For this experiment, we employed a total of 15K images, 3616 of which were positive. COVID-19 images, 10.2k normal X-ray images and 1345 viral pneumonia. Using the Keras data image generator, the images were split into three groups. For training, 10606 images were utilized, 3030 images for validation, and 1517 images for testing. Table 6.3 show all the details.

Results: For Multi-class classification, we have utilized 12 deep learning architectures and compared it with other frameworks that are state of the art. A closer examination of the table 6.4 shows that deep learning architectures are reliable even for multi class classification of the COVID-19 disease. In terms of greatest accuracy, the architecture

Table 6.3: Train Test Split for Multi-Class Classification

Dataset	Total Number of Images	Training	Validation	Testing
Radiography Database (Kaggle)	15153 Normal = 10.2k COVID = 3616 Pneumonia = 1345	10606	3030	1517

Table 6.4: Evaluation Metrics for Multi class Classification

Datasets	Model	Accuracy	Precision	Recall	F1-Score
10* *COVID-19 Radiography Database [20, 71]*	Xception	0.87	0.88	0.82	0.84
	Inception V3	0.85	0.89	0.70	0.75
	Nasnet Large	0.89	0.87	0.87	0.87
	ResNet-50 V2	**0.95**	**0.93**	**0.88**	**0.90**
	Dense Net 121	0.89	0.91	0.84	0.87
	Mobile Net V2	0.91	0.90	0.89	0.89
	VGG-16	0.80	0.83	0.67	0.69
	VGG-19	0.79	0.80	0.69	0.72
	Resnet 50	0.81	0.78	0.89	0.81
	Efficientnet B0	0.67	0.70	0.68	0.65
	Inception Resnet V2	0.90	0.91	0.80	0.84
	Resnet 101 V2	0.91	0.94	0.85	0.89

of Resnet (50-V2) was indeed the best with an accuracy of 95%.

The confusion matrix, loss & accuracy plots & a clustered chart representation for multi-class data set classification results are displayed in figure 6.4, 6.5 and 6.6 respectively and the table 6.5 provides an overview of different approaches and quantitative data for the COVID-19 classification.

Table 6.5: Overview of methods and quantitative results toward COVID-19 classification

Author	Dataset	Method	Results (Accuracy)
Alshazly [15]	SARS COV II	Xception / Densenet 121 / 169	0.88 / 0.87 / 0.85
Nguyen [17]	SARS COV II	Densenet 169 / Resnet 50	0.80 / 0.83
Hasan [18]	SARS COV II	CVR Net	0.78
Martinez [14]	SARS COV II	Densenet 169 / 121	0.87 / 0.85
Proposed	**SARS COV II**	**VGG-16**	**0.98**
Panwar [76]	COVID CT DS GitHub	VGG-19	0.94
Wang [77]	COVID CT DS GitHub	COVID Net	0.90
Proposed	**COVID CT DS GitHub**	**Resnet 101 V2**	**0.96**
Horry [21]	IEEE 8023	VGG-16	0.79
Arellano [78]	IEEE 8023	Densenet 121	0.94
Militante [23]	IEEE 8023	VGG-16	0.95
Proposed	**IEEE 8023**	**Resnet 101 V2**	**0.97**
Proposed	**Radiography DS**	**Resnet 50 V2**	**0.95**
Maguolo [79]	Radiography DS	LOCO	0.79
Enxo [80]	Radiography DS	Resnet 18	0.85

(a) Densenet 121 (b) Resnet 101 V2 (c) Inception Resnet V2

(d) Inception V3 (e) Mobilenet V2 (f) Nasnet Large

(g) Resnet 50 V2 (h) VGG 16 (i) VGG 19

(j) Xception (k) Efficientnet B0 (l) Resnet 50

Figure 6.4: Confusion Matrix for Radiography X-ray Dataset

(a) Training Loss (b) Validation Loss

(c) Training Accuracy (d) Validation Accuracy

Figure 6.5: Loss & Accuracy plots of Radiography Dataset

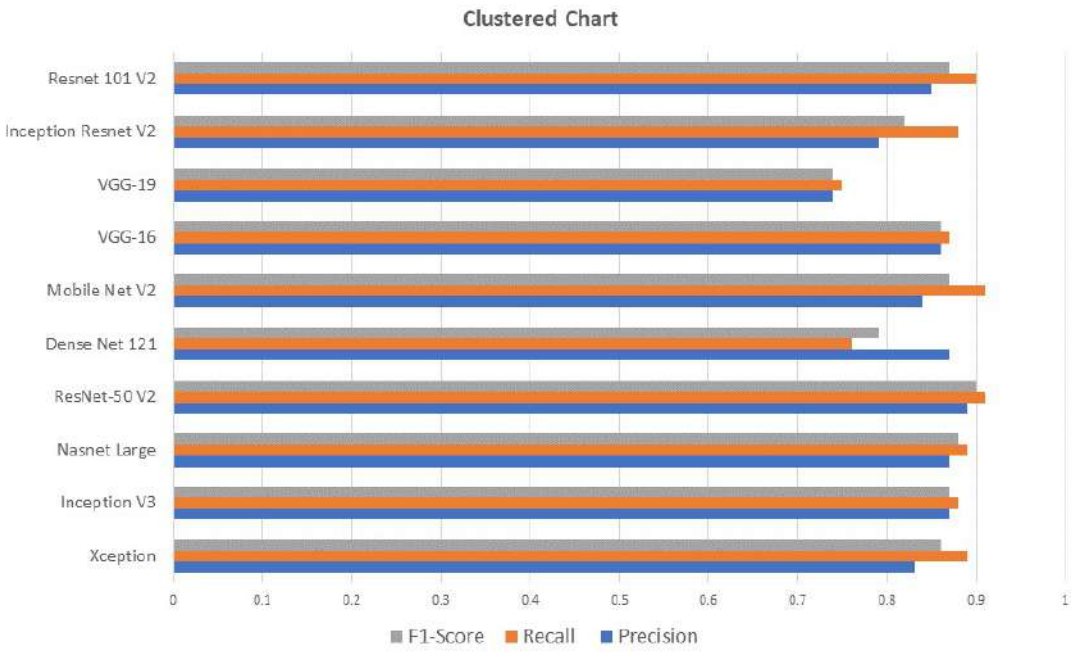

Figure 6.6: Clustered chart representation of Precision, Recall & F1-Score for Multi-class Classification

6.1.3 Binary Class Segmentation's Performance:

The binary class segmentation was implemented on Zenodo dataset. Jaccard Index & F1-Score were the evaluation metrics employed. All the results have been summarized in Table 6.7.

Train Test Split: For binary class segmentation, two classes were segmented: "background and disease." Using the synthetic image creation theme for data augmentation, 1K CT scans were used for this experiment. 500 images for training, 300 for validation and 200 for testing. Table 6.6 show details for the train, test, split.

Table 6.6: Train Test Split for Binary Class Segmentation

Original Number of Images	**After Data Augmentation**	**Training**	**Validation**	**Testing**
20	1000	500	300	200

Results: A close examination of the table 6.7 reveals that all of the architectures with respected backbones showed the maximum Jaccard Index and F1-Score, although the Unet architecture with Mobilenet V2 as encoder (backbone) performed somewhat better attaining an overall F1-Score of 98% on test dataset. The mean F1-Score for each architecture is 97.33% for Unet, 95.33% for PSPNet, 96.83% for Linknet and 92.83% for FPN.

Deep learning frameworks are dependable for segmentation of COVID-19 images. The architecture of Unet was indeed the finest one in terms of the highest F1 score (Fig 6.7).

6.1.4 Multi Class Segmentation's Performance:

The multi class segmentation was carried out on the Zenodo dataset and Medical Segmentation dataset utilizing the background masks, lungs masks and diseases masks for segmentation on the Zenodo Data and the ground glass, consolidation, lungs and background masks for medical segmentation. The evaluation metrics used for the evaluation were Jaccard Index and the F1-Score. Table 6.9 summarizes all the results.

All the available backbones with all architectures were tested and time was taken about one day with one backbone on one architecture on Google Colab.

Table 6.7: Evaluation Metrics for Binary Segmentation

Dataset	Mode	Architecture	Backbone	Jaccard Index	F1-Score
Zenodo	**Binary class**	**Unet**	Efficient Net B3	0.943	0.970
			Mobile Net V2	**0.972**	**0.986**
			Inception Resnet V2	0.970	0.985
			Dense Net 121	0.943	0.970
			SeresNet 101	0.927	0.962
			VGG19	0.915	0.955
		PSPNet	Efficient Net B3	0.927	0.962
			Mobile Net V2	0.932	0.964
			Inception Resnet V2	0.956	0.977
			Dense Net 121	0.957	0.977
			SeresNet 101	0.915	0.955
			VGG19	0.854	0.921
		Linknet	Efficient Net B3	0.921	0.958
			Mobile Net V2	0.961	0.980
			Inception Resnet V2	0.961	0.980
			Dense Net 121	0.915	0.955
			SeresNet 101	0.949	0.973
			VGG19	0.957	0.977
		FPN	Efficient Net B3	0.921	0.958
			Mobile Net V2	0.940	0.969
			Inception Resnet V2	0.959	0.979
			Dense Net 121	0.928	0.962
			SeresNet 101	0.965	0.982
			VGG19	0.886	0.939

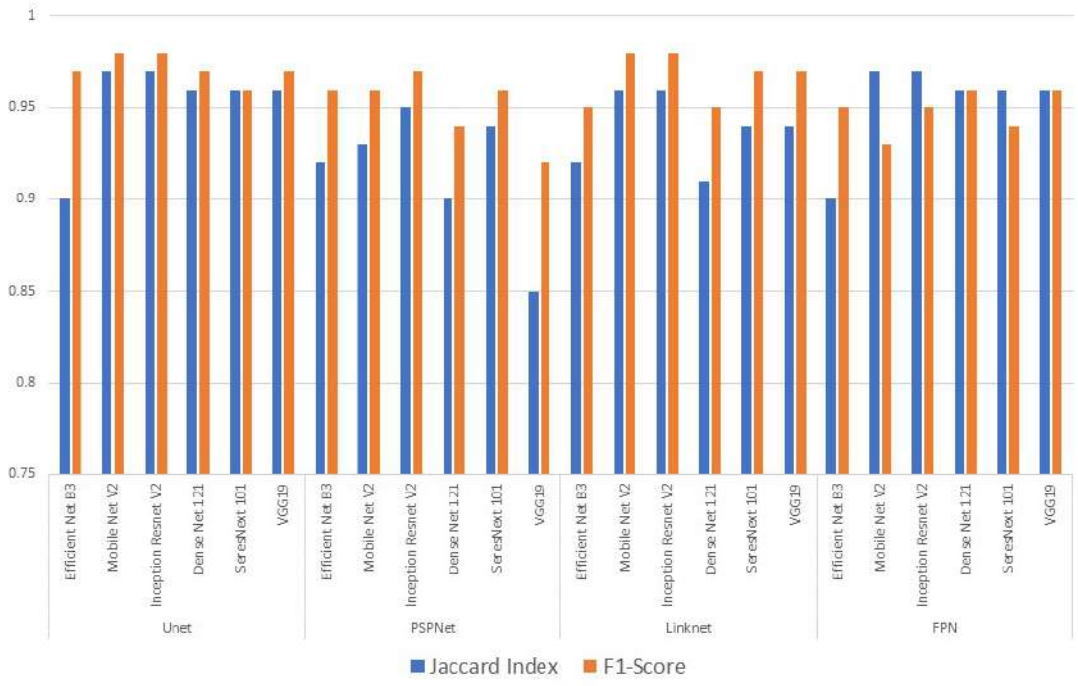

Figure 6.7: Bar Graph representation of Jaccard Index & F1-Score for Binary Class Segmentation

Train Test Split: On the first experiment using the medical segmentation dataset, four classes were segmented: 'ground glass, consolidation, lungs and background" using the medical segmentation dataset. It has two subset dataset "Radiopedia and Medseg". For the radiopedia part, out of 829 slices of images, 580 images were used for training, 124 for validation and 125 for testing. For the Medseg part, 71 images were used for training, 14 for validation and 15 for testing. In total, 651 images were used for training, 138 for validation and 140 for testing. On the second experiment using the zenodo dataset, four classes were segmented "background, right lung, left lung, disease". Using the data image augmentation, 2840 CT images were used for training, 680 for validation and 500 for testing. Details for the train, test, split is mentioned in table 6.8.

Table 6.8: Train Test Split for Multi-Class Segmentation

Dataset	**Original Number of Images**	**Augmentation**	**Training**	**Validation**	**Testing**
Medical Segmentation	829+100	No	580+71	124+14	125+15
Zenodo	20	Yes	2840	680	500

Results: For the medical Segmentation dataset, a detailed analysis in the table 6.9 indicates that all of the architectures with respected backbones had the best F1-Score for multi-class segmentation, while the Linknet architecture with Inception Resnet V2 as encoder performed better with an overall Jaccard Index of 68% and F1-Score of 75% on the test dataset. Each architecture has a mean F1-Score of 72.16% for Linknet, 70.50% for Unet and FPN, and 69.00% for PSPNet. As Linknet is a light deep neural network architecture, it performed well in semantic segmentation, with the capacity to provide real-time performance on both GPUs and embedded devices such as the NVIDIA TX1.

Similarly for the Zenodo Dataset, a deeper examination at the shows that all DL architectures with respected backbones had the best F1-Score, while the FPN architecture with Densenet 121 as encoder excelled at extracting masks for image segmentation on this dataset, with an overall Jaccard Index of 70% F1-Score of 77% on the test dataset. FPN has achieved a mean F1-Score of 73.33%, Unet has a score of 72.66%, Linknet has a score of 69.50%, and PSPNet has a score of 66.33%.

The visual aspect of segmented images is illustrated by Fig 6.8, 6.9. The yellow region is the true positive i.e "an outcome where the model correctly predicts the positive class" Red region is false positive i.e "an outcome where the model incorrectly predicts the

positive class" & green region is false negative i.e " an outcome where the model incorrectly predicts the negative class". A visual representation of the ground vs predicted segmented CT images is demonstrated in figure 6.10 plus a bar graph is demonstrated in figure 6.11 and 6.12.

Finally, the table 6.10 summarizes the proposed model's quantitative results with several baseline classification and segmentation methodologies.

Table 6.9: Evaluation Metrics for Multi class Segmentation

Dataset	Mode	Architecture	Backbone	Jaccard Index	F1-Score
Zenodo	**Multi class**	**Unet**	Efficient Net B3	0.66	0.72
			Mobile Net V2	0.65	0.72
			Inception Resnet V2	0.67	0.73
			Dense Net 121	0.68	0.74
			SeresNet 101	0.69	0.75
			VGG19	0.64	0.70
		PSPNet	Efficient Net B3	0.53	0.60
			Mobile Net V2	0.48	0.54
			Inception Resnet V2	0.64	0.71
			Dense Net 121	0.66	0.72
			SeresNet 101	0.59	0.67
			VGG19	0.67	0.74
		Linknet	Efficient Net B3	0.68	0.74
			Mobile Net V2	0.65	0.71
			Inception Resnet V2	0.69	0.76
			Dense Net 121	0.56	0.63
			SeresNet 101	0.63	0.69
			VGG19	0.58	0.64
		FPN	Efficient Net B3	0.64	0.70
			Mobile Net V2	0.62	0.69
			Inception Resnet V2	0.69	0.76
			Dense Net 121	**0.70**	**0.77**
			SeresNet 101	0.68	0.74
			VGG19	0.68	0.74
Medical Segmentation	**Multi class**	**Unet**	Efficient Net B3	0.64	0.72
			Mobile Net V2	0.63	0.69
			Inception Resnet V2	0.66	0.74
			Dense Net 121	0.60	0.68
			SeresNet 101	0.65	0.73
			VGG19	0.60	0.67
		PSPNet	Efficient Net B3	0.62	0.69
			Mobile Net V2	0.53	0.61
			Inception Resnet V2	0.64	0.72
			Dense Net 121	0.66	0.73
			SeresNet 101	0.66	0.74
			VGG19	0.56	0.64
		Linknet	Efficient Net B3	0.66	0.74
			Mobile Net V2	0.65	0.74
			Inception Resnet V2	**0.68**	**0.75**
			Dense Net 121	0.60	0.68
			SeresNet 101	0.66	0.73
			VGG19	0.61	0.68
		FPN	Efficient Net B3	0.65	0.72
			Mobile Net V2	0.60	0.67
			Inception Resnet V2	0.65	0.72
			Dense Net 121	0.66	0.74
			SeresNet 101	0.65	0.73
			VGG19	0.58	0.65

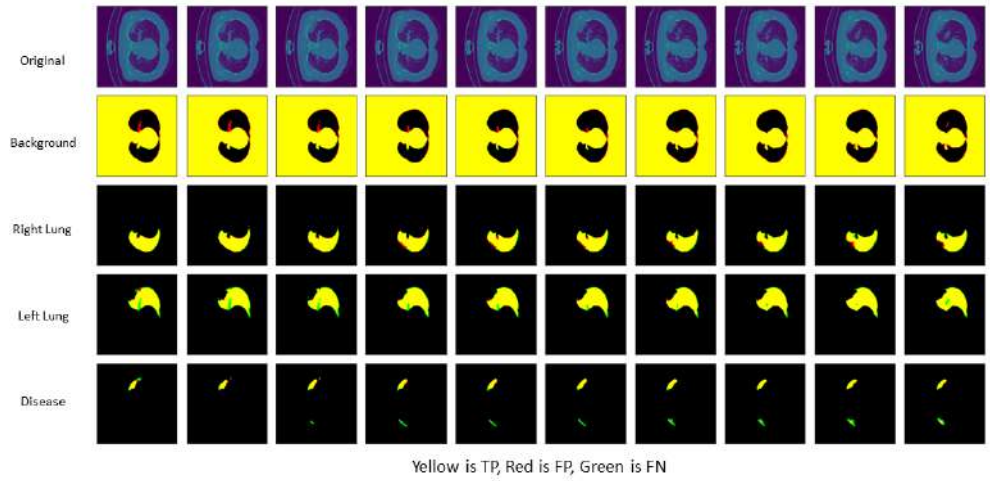

Figure 6.8: Visual Appearance of COVID-19 Segmented Images of Zenodo Dataset

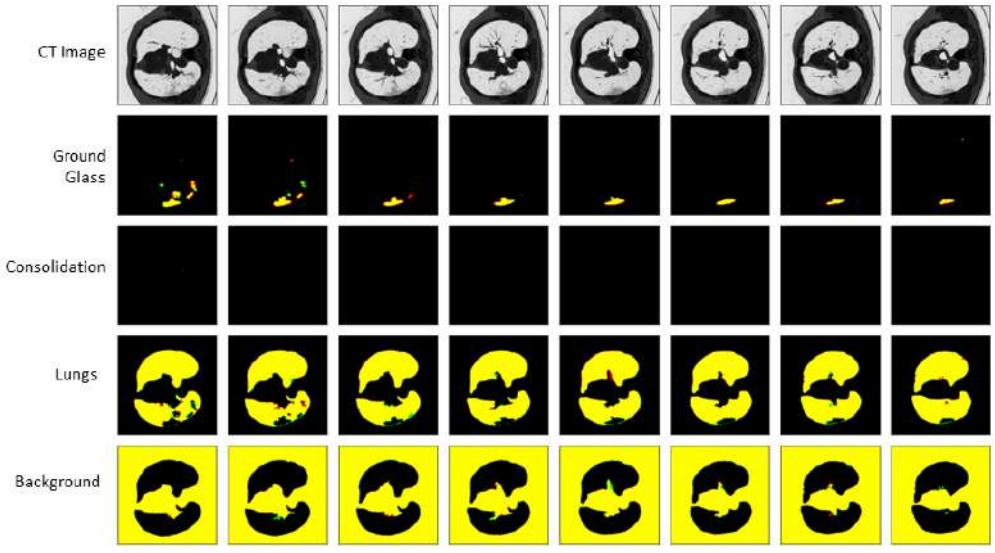

Figure 6.9: Visual Appearance of COVID-19 Segmented Images of Medical Segmentation Dataset

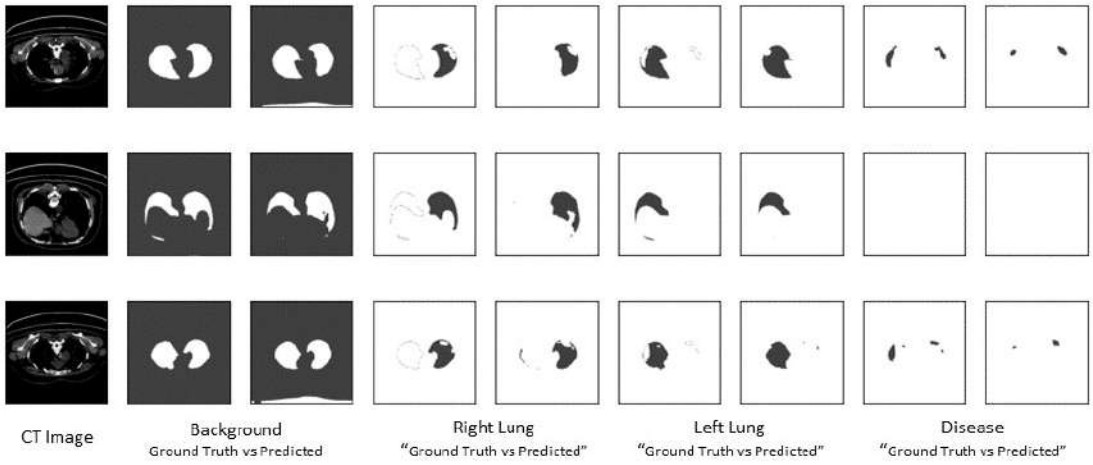

Figure 6.10: Ground Truth vs Predicted of COVID-19 Segmentation

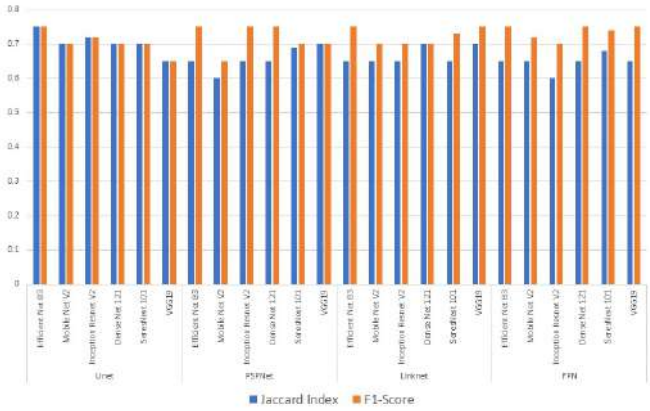

Figure 6.11: Bar Graph representation of Jaccard Index & F1-Score for Multi Class Zenodo Dataset

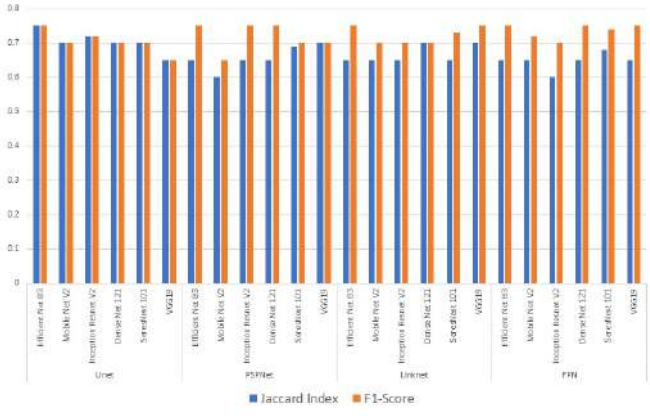

Figure 6.12: Bar Graph representation of Jaccard Index & F1-Score for Multi Class Medical Segmentation Dataset

Table 6.10: Comparison of proposed model to various state of the art baseline classification and segmentation approaches

Mode	Dataset	Author	Method	Results
Classification	**SARS COV II**	H.Alshazly[15]	Xception / Densenet 121-169	0.88 / 0.87 / 0.85
		Nguyen[17]	Densenet 169 / Resnet 50	0.80 / 0.83
		Hassan[18]	CVR Net	0.78
		Martinez[14]	Densenet 169-121	0.87 / 0.75
		Proposed	**VGG-16**	**0.98**
	COVID CT DS	Panwar[76]	VGG-19	0.94
		Wang[25]	COVID Net	0.90
		Mine Amyar[81]	Multi task DL approach	0.94
		Proposed	**Resnet 101 V2**	**0.96**
	IEEE-8023	Horry[21]	VGG-16	0.79
		Arellano[78]	Densenet 121	0.94
		Militante[23]	VGG-16	0.95
		Proposed	**Resnet 101 V2**	**0.97**
	Radiography Database	Maguolo[79]	LOCO	0.79
		Enxo[80]	Resnet 18	0.85
		Proposed	**Resnet 50 V2**	**0.95**
Segmentation	**Zenodo (Multi Class)**	Deng Ping Fan[82]	Inf Net	0.68
		Olaf Ronneberger	Unet	0.70
		Vijay[27]	Segnet	0.50
		Yixin Wang[83]	Hybrid Encoder	0.70
		Proposed	**FPN. Densenet 121**	**0.77**
	Medical Segmentation	Adnan Saood[27]	Unet	0.55
		Proposed	**Linknet. Inception Resnet V2**	**0.75**
	Zenodo (Binary Class)	Dominik[28]	3D Unet	0.76
		Proposed	**Unet. Mobile net V2**	**0.98**

Chapter 7

Conclusion

With COVID-19 now a worldwide danger & killing hundreds of thousands of lives, we provided a detailed comparison of several deep learning architectures for image classification and image segmentation in this research. We suggested various alternative deep learning architectures for image classification and image segmentation to solve the shortage of minimalistic training material and fulfill the efficiency requirement of CAD deployment. In addition, we provide a thorough benchmark that will be beneficial for future studies.

For classification, we trained various deep learning models using deep learning techniques. Using CT and X-ray images, the first experiment makes a binary classification of patients to distinguish between those with COVID-19 and those who do not. We then utilized multi-class classification to distinguish between COVID-19 X-ray images and patients with viral pneumonia and patients with normal X-ray images. It reaches a maximum accuracy of 98 percent for binary class classification and 95 percent for multi class classification, respectively.

We also conducted and trained many deep learning frameworks for binary and multi-class image segmentation. Deep learning architectures are found to be trustworthy for COVID-19 image segmentation, as demonstrated by the results. When it comes to binary segmentation, it achieves the highest F1-scores with 98 percent and 77 percent for multi class segmentation.

According to the findings, all of these deep learning models may be beneficial not only in the classification of COVID-19 CT and X-ray images, but also in the determination of the area of interest of a COVID-19 lesion in the body. These frameworks may assist CAD

systems in diagnosing illness, and they can also assist radiologists in more accurately and quickly identifying disease.

7.1 Future Work

For the future proposals, we can propose:

- Experimenting the proposed framework with other COVID-19 datasets as it become available.
- Using traditional and non-AI techniques to evaluate the proposed framework.
- In the proposed segmentation architecture, investigating the effects of higher input resolution and different types of other encoders.
- Exploring the effect of higher input resolution for classification.

References

[1] Junaid Shuja, Eisa Alanazi, Waleed Alasmary, and Abdulaziz Alashaikh. Covid-19 open source data sets: A comprehensive survey. *Applied Intelligence*, pages 1–30, 2020.

[2] MJ Keeling, TD Hollingsworth, and JM Read. The efficacy of contact tracing for the containment of the 2019 novel coronavirus (covid-19). medrxiv 2020. 02.14. 20023036. *Google Scholar*, 2020.

[3] Noreen Iftikhar. Breathtaking lungs: Their function and anatomy, 2018. URL https://www.healthline.com/human-body-maps/lung.

[4] Lungs anatomy. URL https://www.enchantedlearning.com/subjects/anatomy/lungs/.

[5] Neha Phatak. Coronavirus and covid-19: What you should know, 2021. URL https://www.webmd.com/lung/coronavirus.

[6] Cleveland Clinic. Coronavirus, covid-19, 2020. URL https://my.clevelandclinic.org/health/diseases/21214-coronavirus-covid-19.

[7] Nicole Jawerth. A window inside the body and covid-19, year = 2020, url = https://www.iaea.org/bulletin/infectious-diseases/a-window-inside-the-body-and-covid-19.

[8] Chih-Cheng Lai, Yen Hung Liu, Cheng-Yi Wang, Ya-Hui Wang, Shun-Chung Hsueh, Muh-Yen Yen, Wen-Chien Ko, and Po-Ren Hsueh. Asymptomatic carrier state, acute respiratory disease, and pneumonia due to severe acute respiratory syndrome coronavirus 2 (sars-cov-2): Facts and myths. *Journal of Microbiology, Immunology and Infection*, 53(3):404–412, 2020.

[9] Sebastian Hoehl, Holger Rabenau, Annemarie Berger, Marhild Kortenbusch, Jindrich Cinatl, Denisa Bojkova, Pia Behrens, Boris Böddinghaus, Udo Götsch, Frank Naujoks, et al. Evidence of sars-cov-2 infection in returning travelers from wuhan, china. *New England Journal of Medicine*, 382(13):1278–1280, 2020.

[10] Tuan D Pham. A comprehensive study on classification of covid-19 on computed tomography with pretrained convolutional neural networks. *Scientific Reports*, 10 (1):1–8, 2020.

[11] Tulin Ozturk, Muhammed Talo, Eylul Azra Yildirim, Ulas Baran Baloglu, Ozal Yildirim, and U Rajendra Acharya. Automated detection of covid-19 cases using deep neural networks with x-ray images. *Computers in biology and medicine*, 121: 103792, 2020.

[12] Asif Iqbal Khan, Junaid Latief Shah, and Mohammad Mudasir Bhat. Coronet: A deep neural network for detection and diagnosis of covid-19 from chest x-ray images. *Computer Methods and Programs in Biomedicine*, 196:105581, 2020.

[13] Tanvir Mahmud, Md Awsafur Rahman, and Shaikh Anowarul Fattah. Covxnet: A multi-dilation convolutional neural network for automatic covid-19 and other pneumonia detection from chest x-ray images with transferable multi-receptive feature optimization. *Computers in biology and medicine*, 122:103869, 2020.

[14] Alejandro R Martinez. Classification of covid-19 in ct scans using multi-source transfer learning. *arXiv preprint arXiv:2009.10474*, 2020.

[15] Hammam Alshazly, Christoph Linse, Erhardt Barth, and Thomas Martinetz. Explainable covid-19 detection using chest ct scans and deep learning. *Sensors*, 21(2): 455, 2021.

[16] Bin Liu, Xiaoxue Gao, Mengshuang He, Lin Liu, and Guosheng Yin. A fast online covid-19 diagnostic system with chest ct scans. In *Proceedings of KDD*, volume 2020, 2020.

[17] DMH Nguyen, DM Nguyen, H Vu, BT Nguyen, F Nunnari, and D Sonntag. An attention mechanism with multiple knowledge sources for covid-19 detection from ct images. 2020.

[18] Md Hasan, Md Alam, Md Elahi, E Toufick, Shidhartho Roy, Sifat Redwan Wahid, et al. Cvr-net: A deep convolutional neural network for coronavirus recognition from chest radiography images. *arXiv preprint arXiv:2007.11993*, 2020.

[19] Xiang Yu, Shui-Hua Wang, and Yu-Dong Zhang. Cgnet: A graph-knowledge embedded convolutional neural network for detection of pneumonia. *Information Processing & Management*, 58(1):102411, 2021.

[20] Muhammad EH Chowdhury, Tawsifur Rahman, Amith Khandakar, Rashid Mazhar, Muhammad Abdul Kadir, Zaid Bin Mahbub, Khandakar Reajul Islam, Muhammad Salman Khan, Atif Iqbal, Nasser Al Emadi, et al. Can ai help in screening viral and covid-19 pneumonia? *IEEE Access*, 8:132665–132676, 2020.

[21] Michael J Horry, Subrata Chakraborty, Manoranjan Paul, Anwaar Ulhaq, Biswajeet Pradhan, Manas Saha, and Nagesh Shukla. Covid-19 detection through transfer learning using multimodal imaging data. *IEEE Access*, 8:149808–149824, 2020.

[22] Siti Raihanah Abdani, Mohd Asyraf Zulkifley, and Nuraisyah Hani Zulkifley. A lightweight deep learning model for covid-19 detection. In *2020 IEEE Symposium on Industrial Electronics & Applications (ISIEA)*, pages 1–5. IEEE, 2020.

[23] Sammy V Militante, Nanette V Dionisio, and Brandon G Sibbaluca. Pneumonia and covid-19 detection using convolutional neural networks. In *2020 Third International Conference on Vocational Education and Electrical Engineering (ICVEE)*, pages 1–6. IEEE, 2020.

[24] Prabira Kumar Sethy, Santi Kumari Behera, Pradyumna Kumar Ratha, and Preesat Biswas. Detection of coronavirus disease (covid-19) based on deep features and support vector machine. 2020.

[25] Linda Wang, Zhong Qiu Lin, and Alexander Wong. Covid-net: A tailored deep convolutional neural network design for detection of covid-19 cases from chest x-ray images. *Scientific Reports*, 10(1):1–12, 2020.

[26] Narges Saeedizadeh, Shervin Minaee, Rahele Kafieh, Shakib Yazdani, and Milan Sonka. Covid tv-unet: Segmenting covid-19 chest ct images using connectivity imposed unet. *Computer Methods and Programs in Biomedicine Update*, page 100007, 2021.

[27] Adnan Saood and Iyad Hatem. Covid-19 lung ct image segmentation using deep learning methods: U-net versus segnet. *BMC Medical Imaging*, 21(1):1–10, 2021.

[28] Dominik Müller, Iñaki Soto Rey, and Frank Kramer. Automated chest ct image segmentation of covid-19 lung infection based on 3d u-net. *arXiv preprint arXiv:2007.04774*, 2020.

[29] Amine Amyar, Romain Modzelewski, Hua Li, and Su Ruan. Multi-task deep learning based ct imaging analysis for covid-19 pneumonia: Classification and segmentation. *Computers in Biology and Medicine*, 126:104037, 2020.

[30] Athanasios Voulodimos, Eftychios Protopapadakis, Iason Katsamenis, Anastasios Doulamis, and Nikolaos Doulamis. Deep learning models for covid-19 infected area segmentation in ct images. *medRxiv*, 2020.

[31] Kai Gao, Jianpo Su, Zhongbiao Jiang, Ling-Li Zeng, Zhichao Feng, Hui Shen, Pengfei Rong, Xin Xu, Jian Qin, Yuexiang Yang, et al. Dual-branch combination network (dcn): Towards accurate diagnosis and lesion segmentation of covid-19 using ct images. *Medical image analysis*, 67:101836, 2021.

[32] Yu Qiu, Yun Liu, Shijie Li, and Jing Xu. Miniseg: An extremely minimum network for efficient covid-19 segmentation, 2021.

[33] Alex Noel Joseph Raj, Haipeng Zhu, Asiya Khan, Zhemin Zhuang, Zengbiao Yang, Vijayalakshmi GV Mahesh, and Ganesan Karthik. Adid-unet—a segmentation model for covid-19 infection from lung ct scans. *PeerJ Computer Science*, 7:e349, 2021.

[34] Tongxue Zhou, Stéphane Canu, and Su Ruan. Automatic covid -19 ct segmentation using u-net integrated spatial and channel attention mechanism. *International Journal of Imaging Systems and Technology*, 31(1):16–27, Nov 2020. ISSN 1098-1098. doi: 10.1002/ima.22527. URL http://dx.doi.org/10.1002/ima.22527.

[35] Omar Elharrouss, Nandhini Subramanian, and Somaya Al-Maadeed. An encoder-decoder-based method for covid-19 lung infection segmentation, 2020.

[36] Yu-Huan Wu, Shang-Hua Gao, Jie Mei, Jun Xu, Deng-Ping Fan, Rong-Guo Zhang, and Ming-Ming Cheng. Jcs: An explainable covid-19 diagnosis system

by joint classification and segmentation. *IEEE Transactions on Image Processing*, 30:3113–3126, 2021. ISSN 1941-0042. doi: 10.1109/tip.2021.3058783. URL http://dx.doi.org/10.1109/TIP.2021.3058783.

[37] Levity. URL https://levity.ai/.

[38] Yann LeCun, Yoshua Bengio, and Geoffrey Hinton. Deep learning. *nature*, 521 (7553):436–444, 2015.

[39] Ziwei Zhang, Peng Cui, and Wenwu Zhu. Deep learning on graphs: A survey. *IEEE Transactions on Knowledge and Data Engineering*, 2020.

[40] Ajay Shrestha and Ausif Mahmood. Review of deep learning algorithms and architectures. *IEEE Access*, 7:53040–53065, 2019.

[41] Maryam M Najafabadi, Flavio Villanustre, Taghi M Khoshgoftaar, Naeem Seliya, Randall Wald, and Edin Muharemagic. Deep learning applications and challenges in big data analytics. *Journal of big data*, 2(1):1–21, 2015.

[42] Ian Goodfellow, Yoshua Bengio, and Aaron Courville. *Deep learning*. MIT press, 2016.

[43] Connor Shorten, Taghi M Khoshgoftaar, and Borko Furht. Deep learning applications for covid-19. *Journal of big Data*, 8(1):1–54, 2021.

[44] Luca Brunese, Francesco Mercaldo, Alfonso Reginelli, and Antonella Santone. Explainable deep learning for pulmonary disease and coronavirus covid-19 detection from x-rays. *Computer Methods and Programs in Biomedicine*, 196:105608, 2020.

[45] Mohammad Jamshidi, Ali Lalbakhsh, Jakub Talla, Zdeněk Peroutka, Farimah Hadjilooei, Pedram Lalbakhsh, Morteza Jamshidi, Luigi La Spada, Mirhamed Mirmozafari, Mojgan Dehghani, et al. Artificial intelligence and covid-19: deep learning approaches for diagnosis and treatment. *Ieee Access*, 8:109581–109595, 2020.

[46] Mohammad Shorfuzzaman and M Shamim Hossain. Metacovid: A siamese neural network framework with contrastive loss for n-shot diagnosis of covid-19 patients. *Pattern recognition*, 113:107700, 2021.

[47] Machine learning and deep learning 101 - networking technologies. https:/www.netcloud.com/blog/machine-learning-and-deep-learning-101/.

[48] Alex Krizhevsky, Ilya Sutskever, and Geoffrey E Hinton. Imagenet classification with deep convolutional neural networks. *Advances in neural information processing systems*, 25:1097–1105, 2012.

[49] Dog breed identification with fine tuning of pre-trained models. https:/www.ijrte.org/wp-content/uploads/papers/v8i2S11/B14640982S1119.pdf.

[50] Convolution neural network for image processing — using keras | by angel das | towards data science. https:/towardsdatascience.com/convolution-neural-network-for-image-processing-using-keras-dc3429056306, .

[51] Neural convolutional layers. https://m-alcu.github.io/blog/2018/01/13/neural-layers/.

[52] 9.5 neural networks | analysis of 2019 kaggle ml & ds survey. http://machinelearningintro.uwesterr.de/MlAlgoNN.html.

[53] Understand the architecture of cnn | by kousai smeda | towards data science. https://towardsdatascience.com/understand-the-architecture-of-cnn-90a25e244c7.

[54] Devi Frossard. Vgg in tensorflow. URL https://www.cs.toronto.edu/~frossard/post/vgg16/.

[55] Karen Simonyan and Andrew Zisserman. Very deep convolutional networks for large-scale image recognition. *arXiv preprint arXiv:1409.1556*, 2014.

[56] Gao Huang, Zhuang Liu, Laurens Van Der Maaten, and Kilian Q Weinberger. Densely connected convolutional networks. In *Proceedings of the IEEE conference on computer vision and pattern recognition*, pages 4700–4708, 2017.

[57] Resnet (34, 50, 101): Residual cnns for image classification tasks. https://neurohive.io/en/popular-networks/resnet/.

[58] Kaiming He, Xiangyu Zhang, Shaoqing Ren, and Jian Sun. Deep residual learning for image recognition. corr abs/1512.03385 (2015), 2015.

[59] Review: Mobilenetv2 — light weight model (image classification) | by sik-ho tsang | towards data science. https://towardsdatascience.com/

review-mobilenetv2-light-weight-model-image-classification-8febb490e61c,
.

[60] François Chollet. Xception: deep learning with depthwise separable convolutions. corr abs/1610.02357 (2016). *arXiv preprint arXiv:1610.02357*, 2016.

[61] Xception: Implementing from scratch using tensorflow | by arjun sarkar | towards data science. https://towardsdatascience.com/xception-from-scratch-using-tensorflow-even-better-than-inception-940fb231ced9.

[62] Christian Szegedy, Sergey Ioffe, Vincent Vanhoucke, and Alex Alemi. Inception-v4, inception-resnet and the impact of residual connections on learning (2016). *arXiv preprint arXiv:1602.07261*, 2016.

[63] Inception-resnet-v2-b explained | papers with code. https://paperswithcode.com/method/inception-resnet-v2-b.

[64] The network architecture of efficientnet. it can output a feature map... | download scientific diagram. https://www.researchgate.net/figure/The-network-architecture-of-EfficientNet-It-can-output-a-feature-map-with-deep-s fig3_349299852.

[65] Review: Nasnet — neural architecture search network (image classification) | by sik-ho tsang | medium. https://sh-tsang.medium.com/review-nasnet-neural-architecture-search-network-image-classification-23139ea042
.

[66] qubvel/segmentation_models: Segmentation models with pretrained backbones. keras and tensorflow keras. https://github.com/qubvel/segmentation_models.

[67] Review of deep learning: concepts, cnn architectures, challenges, applications, future directions | journal of big data | full text. https://journalofbigdata.springeropen.com/articles/10.1186/s40537-021-00444-8, .

[68] Yoshua Bengio, Yann Lecun, and Geoffrey Hinton. Deep learning for ai. *Communications of the ACM*, 64(7):58–65, 2021.

[69] Plamen Angelov and Eduardo Almeida Soares. Sars-cov-2 ct-scan dataset: A large dataset of real patients ct scans for sars-cov-2 identification. *MedRxiv*, 2020.

[70] Xingyi Yang, Xuehai He, Jinyu Zhao, Yichen Zhang, Shanghang Zhang, and Pengtao Xie. Covid-ct-dataset: a ct scan dataset about covid-19. *arXiv preprint arXiv:2003.13865*, 2020.

[71] Tawsifur Rahman, Amith Khandakar, Yazan Qiblawey, Anas Tahir, Serkan Kiranyaz, Saad Bin Abul Kashem, Mohammad Tariqul Islam, Somaya Al Maadeed, Susu M Zughaier, Muhammad Salman Khan, et al. Exploring the effect of image enhancement techniques on covid-19 detection using chest x-ray images. *Computers in biology and medicine*, 132:104319, 2021.

[72] Joseph Paul Cohen, Paul Morrison, Lan Dao, Karsten Roth, Tim Q Duong, and Marzyeh Ghassemi. Covid-19 image data collection: Prospective predictions are the future. *arXiv preprint arXiv:2006.11988*, 2020.

[73] Covid-19 ct segmentation dataset. 2020. URL http://medicalsegmentation.com/covid19/.

[74] Covid-19 ct lung and infection segmentation dataset. 2020. URL https://zenodo.org/record/3757476#.YWvaavpBzIU.

[75] Confusion matrix for your multi-class machine learning model | by joydwip mohajon | towards data science. https://towardsdatascience.com/confusion-matrix-for-your-multi-class-machine-learning-model-ff9aa3bf7826, .

[76] Harsh Panwar, PK Gupta, Mohammad Khubeb Siddiqui, Ruben Morales-Menendez, Prakhar Bhardwaj, and Vaishnavi Singh. A deep learning and grad-cam based color visualization approach for fast detection of covid-19 cases using chest x-ray and ct-scan images. *Chaos, Solitons & Fractals*, 140:110190, 2020.

[77] Zhao Wang, Quande Liu, and Qi Dou. Contrastive cross-site learning with redesigned net for covid-19 ct classification. *IEEE Journal of Biomedical and Health Informatics*, 24(10):2806–2813, 2020.

[78] Matías Cam Arellano and Oscar E Ramos. Deep learning model to identify covid-19 cases from chest radiographs. In *2020 IEEE XXVII International Conference on Electronics, Electrical Engineering and Computing (INTERCON)*, pages 1–4. IEEE, 2020.

[79] G Maguolo and L Nanni. A critic evaluation of methods for covid-19 automatic detection from x-ray images. arxiv 2020. *arXiv preprint arXiv:2004.12823*, 2020.

[80] Enzo Tartaglione, Carlo Alberto Barbano, Claudio Berzovini, Marco Calandri, and Marco Grangetto. Unveiling covid-19 from chest x-ray with deep learning: a hurdles race with small data. *International Journal of Environmental Research and Public Health*, 17(18):6933, 2020.

[81] Zahra Nabizadeh-Shahre-Babak, Nader Karimi, Pejman Khadivi, Roshanak Roshandel, Ali Emami, and Shadrokh Samavi. Detection of covid-19 in x-ray images by classification of bag of visual words using neural networks. *Biomedical Signal Processing and Control*, 68:102750, 2021.

[82] Deng-Ping Fan, Tao Zhou, Ge-Peng Ji, Yi Zhou, Geng Chen, Huazhu Fu, Jianbing Shen, and Ling Shao. Inf-net: Automatic covid-19 lung infection segmentation from ct images. *IEEE Transactions on Medical Imaging*, 39(8):2626–2637, 2020.

[83] Jun Ma, Yixin Wang, Xingle An, Cheng Ge, Ziqi Yu, Jianan Chen, Qiongjie Zhu, Guoqiang Dong, Jian He, Zhiqiang He, et al. Toward data-efficient learning: A benchmark for covid-19 ct lung and infection segmentation. *Medical physics*, 48(3): 1197–1210, 2021.